Unilateral electrical stimulation of rat locus coeruleus elicits bilateral response of norepinephrine neurons and sustained activation of medial prefrontal cortex

Aude Marzo, ^{1*} Nelson K. Totah, ^{1*} Ricardo M. Neves, ¹ Nikos K. Logothetis, ^{1,2} and Oxana Eschenko ¹ Max Planck Institute for Biological Cybernetics, Tübingen, Germany; and ² Centre for Imaging Sciences, Biomedical Imaging Institute, University of Manchester, Manchester, United Kingdom

Submitted 30 December 2013; accepted in final form 19 March 2014

Marzo A, Totah NK, Neves RM, Logothetis NK, Eschenko O. Unilateral electrical stimulation of rat locus coeruleus elicits bilateral response of norepinephrine neurons and sustained activation of medial prefrontal cortex. J Neurophysiol 111: 2570-2588, 2014. First published March 26, 2014; doi:10.1152/jn.00920.2013.—The brain stem nucleus locus coeruleus (LC) is thought to modulate cortical excitability by norepinephrine (NE) release in LC forebrain targets. The effects of LC burst discharge, typically evoked by a strong excitatory input, on cortical ongoing activity are poorly understood. To address this question, we combined direct electrical stimulation of LC (LC-DES) with extracellular recording in LC and medial prefrontal cortex (mPFC), an important cortical target of LC. LC-DES consisting of single pulses (0.1-0.5 ms, 0.01-0.05 mA) or pulse trains (20-50 Hz, 50-200 ms) evoked short-latency excitatory and inhibitory LC responses bilaterally as well as a delayed rebound excitation occurring \sim 100 ms after stimulation offset. The pulse trains, but not single pulses, reliably elicited mPFC activity change, which was proportional to the stimulation strength. The firing rate of $\sim 50\%$ of mPFC units was significantly modulated by the strongest LC-DES. Responses of mPFC putative pyramidal neurons included fast (~100 ms), transient (~100-200 ms) inhibition (10% of units) or excitation (13%) and delayed (\sim 500 ms), sustained (\sim 1 s) excitation (26%). The sustained spiking resembled NE-dependent mPFC activity during the delay period of working memory tasks. Concurrently, the lowfrequency (0.1-8 Hz) power of the local field potential (LFP) decreased and high-frequency (>20 Hz) power increased. Overall, the DES-induced LC firing pattern resembled the naturalistic biphasic response of LC-NE neurons to alerting stimuli and was associated with a shift in cortical state that may optimize processing of behaviorally relevant events.

arousal; cortical excitability; direct electrical stimulation; locus coeruleus; neuromodulation

THE LEVEL OF NOREPINEPHRINE (NE) in the brain modulates a variety of cognitive capacities such as perception, attention, learning, working memory, and behavioral flexibility (Sara 2009). The brain stem neuromodulatory nucleus locus coeruleus (LC) is a major source of NE in the forebrain. Being a part of a so-called diffuse ascending arousal system, LC terminals are widely spread throughout the brain (Jones and Moore 1977; Lindvall et al. 1978) and have both synaptic and volume transmission (Beaudet and Descarries 1978). The anatomical organization of the LC-NE system and physiological properties of LC-NE neurons underlie a broad range of neuromodulatory effects of NE that are expressed with diverse specificity at different timescales, from milliseconds to hours

(Moore and Bloom 1979). The global-local neural interactions between widely distributed LC-NE efferents and excitatory/ inhibitory circuits in the LC projection targets result in event-specific local processing optimization (Aston-Jones and Cohen 2005; Berridge and Waterhouse 2003; Sara 2009), yet relatively little is known about these interactions, as well as about the behavioral consequences of LC event-triggered phasic activation.

The involvement of the LC-NE system in regulating brain functions such as sleep/awake cycle, vigilance state, or modulation and optimization of information processing is well recognized (Aston-Jones and Cohen 2005; Berridge 2008; Berridge and Waterhouse 2003). A relatively recent hypothesis focuses on the attempt to explain the effects of LC phasic activation, or burst discharge of LC-NE neurons (as opposed to tonic fluctuation of the firing rate). LC burst discharge, which is the most efficient for NE release (Berridge and Abercrombie 1999; Devoto et al. 2005; Florin-Lechner et al. 1996), can be elicited by nonspecific alerting external (Cedarbaum and Aghajanian 1978; Foote et al. 1980) or internal (Groves et al. 2005) stimuli but also by conditioned stimuli or internally generated outcomes of the decision-making processes related to performance of a goal-directed behavior (Aston-Jones et al. 1994; Bouret and Richmond 2009; Bouret and Sara 2004). The current theory suggests that phasic LC activation may serve as an "interrupt" or "reset" signal in relation to the behaviorally relevant events and that the concurrent NE release in the multiple forebrain targets of LC facilitates dynamic reorganization of the local neural networks according to the ongoing behavioral demands (Bouret and Sara 2005; Dayan and Yu 2006; Hermans et al. 2011). In all of the diverse behavioral instances triggering LC phasic discharge, the associated NE release may alter properties of large-scale neural populations immediately after a salient external or internal event. However, experimental characterization of the temporal and spatial discreteness of NE effects has always presented a challenge, and it remains poorly understood.

Earlier studies have demonstrated that bursts of LC activity increase the signal-to-noise ratio of thalamic and cortical sensory-evoked responses (Bouret and Sara 2002; Devilbiss et al. 2006; Devilbiss and Waterhouse 2011; Kayama and Sato 1982; Lecas 2004; Sato et al. 1989; Snow et al. 1999). Such beneficial impact of LC phasic activity on sensory information processing in the upstream LC targets may result from a reduced afterhyperpolarization or decreased background firing of target neurons (see Sara 2009 for review). Much less is known about the physiological effects of phasic NE release in associative cortical regions, such as the medial prefrontal

^{*} A. Marzo and N. K. Totah contributed equally to this work.

Address for reprint requests and other correspondence: O. Eschenko, Max

Planck Inst. for Biological Cybernetics, Spemannstrasse 38, Tübingen

D-72076, Germany (e-mail: oxana.eschenko@tuebingen.mpg.de).

cortex (mPFC), that are critical for higher-order cognitive functions. The LC phasic response to a salient stimulus is thought to beneficially contribute to attention, working memory, or behavioral flexibility by affecting the prefrontal NE neurotransmission (Arnsten 2011; Aston-Jones and Gold 2009; Berridge and Waterhouse 2003; Sara 2009). Nonetheless, to the best of our knowledge, the effects of phasic NE release on the responsiveness of mPFC neurons has never been described in detail.

To study the effective connectivity of LC and its ability to shape and optimize cortical activity with fine temporal resolution, the application of methods allowing fast modulation of local LC activity, for example, direct electrical stimulation (DES), is of obvious advantage. DES is a classical experimental tool that can robustly excite the axons of a stimulated brain region and therefore modulate its output at the temporal resolution of milliseconds (Borchers et al. 2012; Butovas and Schwarz 2003; Cohen and Newsome 2004; Grill et al. 2004; Histed et al. 2009; Ranck 1975; Tehovnik et al. 2006). Earlier studies demonstrated that LC-DES caused EEG desynchronization (Dringenberg and Vanderwolf 1997). At the single-unit level, both excitatory and inhibitory effects in cortex due to LC stimulation have been reported (Dillier et al. 1978; Mantz et al. 1988; Olpe et al. 1980; Phillis and Kostopoulos 1977; Sato et al. 1989). Importantly, the response of LC-NE neurons to DES—conducted with highly variable stimulation parameters—was not monitored, and therefore the effects of LC-DES on cortical activity cannot be easily compared to the cortical effects of the naturalistic stimulus-evoked bursts of LC firing. It follows that a comprehensive study of the effects of multiple stimulation conditions on the LC-NE neurons themselves, as well as on cortical ongoing activity, is a necessary step forward in elucidating the role of the LC-NE system as cortical state modulator.

We sought to characterize neural responses in both the modulating (LC) and the target (mPFC) structure under a variety of LC stimulation conditions. Our results show that injection of a threshold current in one LC typically evokes a bilateral LC discharge followed by inhibition. In mPFC, mild LC stimulation appears to elicit excitation in a substantially greater proportion and inhibition in a smaller proportion of neurons. The resulting shift in excitation/inhibition balance is reflected in the local field potential (LFP), which indicated an activated cortical state. The responsiveness of mPFC neurons was proportional to the degree of cortical activation elicited by LC-DES. These findings suggest that LC phasic activity may rapidly modulate the mPFC state for optimal processing of behaviorally relevant events.

METHODS

Animals. Nineteen male Sprague-Dawley rats (200–350 g, Charles River) were used in the study. All experimental procedures were approved by and carried out in accordance with the local authorities (Regierungspräsidium) and were in full compliance with the European Parliament and Council Directive 2010/63/EU on the protection of animals used for experimental and other scientific purposes.

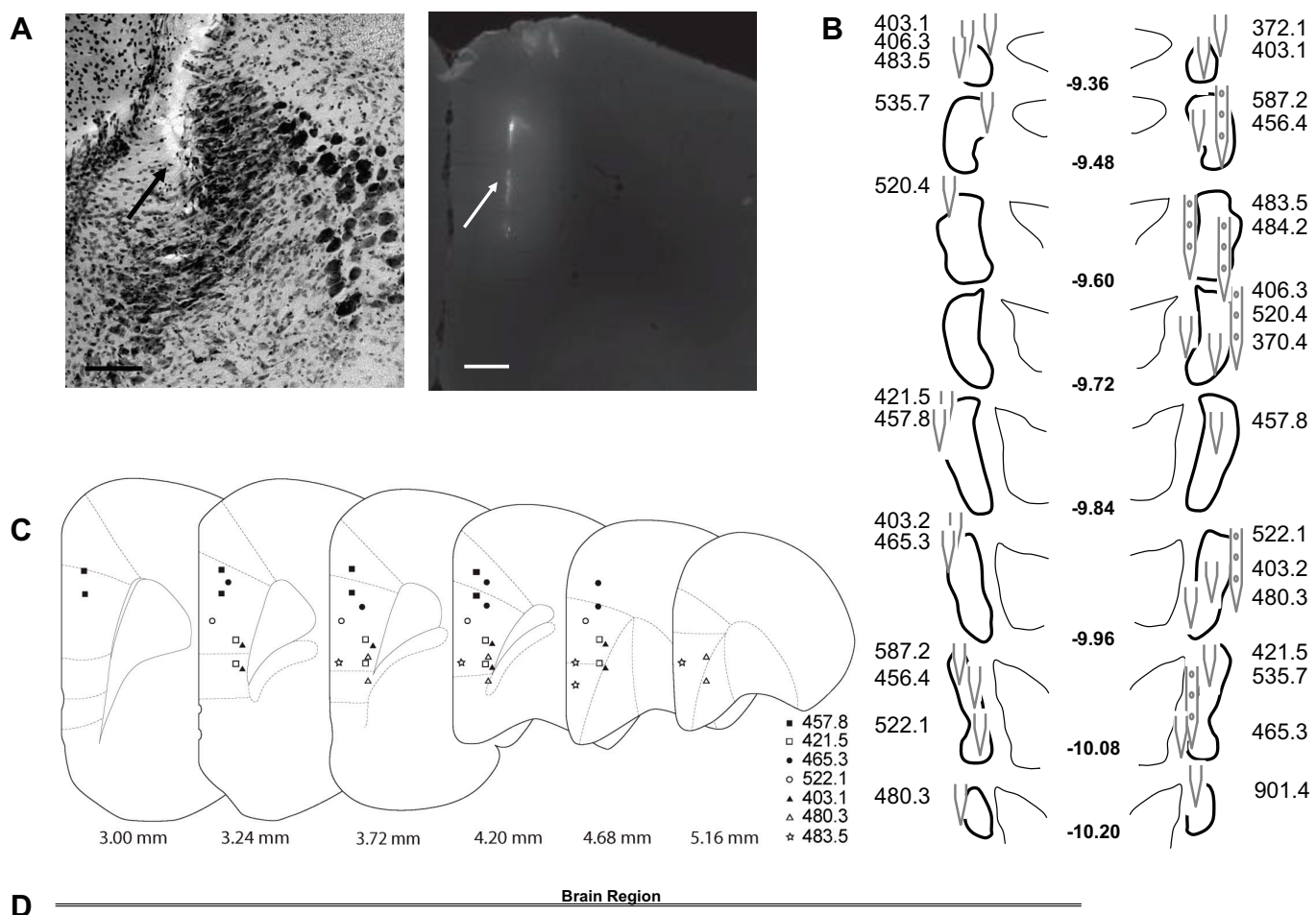
Anesthesia. Experiments were performed under urethane anesthesia (1.5 g/kg ip). The depth of anesthesia was monitored by ensuring lack of responses to mildly noxious stimuli (pinch of hind paw). Typically, a single injection of urethane was sufficient to maintain a deep level of anesthesia for up to 10 h; drug supplements (10% of the initial dose) were given as needed. The rats' heart rate and blood oxygen-

ation were monitored with a pulse oximeter (Nonin 8600V, Nonin Medical, Plymouth, MN), and oxygen was provided to maintain the blood oxygenation level above 80%. The body temperature was maintained at 37°C throughout the experiment.

Surgery and electrode placement. A fully anesthetized rat was fixed in a stereotaxic frame. The head angle was set at 0°. The skull was exposed, and local anesthetic (Lidocard 2%, B. Braun, Melsungen, Germany) was applied on the skin edges to additionally numb the skin. Burr holes were made above the electrode placement, and dura mater was removed. The electrodes were placed in the target brain areas with stereotaxic micromanipulators (David Kopf Instruments, Tujunga, CA); the final adjustment of the electrode position was guided by online monitoring of neural activity. Thirty-two-channel silicone-based microelectrode arrays (NeuroNexus Technologies, Ann Arbor, MI) were used for mPFC recordings. The array consisted of four shanks (0.4-mm spacing) with two tetrodes on each shank (0.5-mm distance between tetrodes). The electrode array was placed in the mPFC such that four shanks would cover ~1.2 mm in the anterior-posterior direction (~3-4 mm anterior to bregma); all four shanks were placed ~ 0.5 mm lateral to the midline targeting deep cortical layers and lowered at depth $\sim 3.5-4.0$ mm from the brain surface. At least one electrode contact of the array was used for a wide-band (0.1 Hz-8 kHz) recording. For LC simultaneous recording and stimulation we used custom-made glass-coated iridium electrodes (0.075-mm wire diameter; impedance $\sim 300-400 \text{ k}\Omega$). In some experiments, 16-channel linear microelectrode arrays (NeuroNexus Technologies) with 0.1-mm spacing between the electrode contacts were used for multisite recording and stimulation within the LC. The LC electrode was implanted at an angle of 15° at the following coordinates: 4.0-4.2 mm posterior to lambda, 1.2 mm lateral to the midline, 5.5–6.2 mm deep from the brain surface. For recording in the contralateral LC, a single tungsten recording electrode (FHC, Bowdoin, ME) was positioned with the same coordinates. A reconstruction of all recording sites is shown in Fig. 1. A silver wire inserted in the muscle tissue on the rat's head served as the ground for both recording and stimulation.

Direct electrical stimulation and recordings. For simultaneous recording/stimulation, we used a custom-made glass-coated iridium electrode or one contact of the linear array (NeuroNexus Technologies) placed in the LC core (Fig. 1). A custom-built electric switch between the recording and stimulation modes was software controlled such that the stimulation mode was switched on 1 ms before LC-DES and switched off immediately after stimulation offset. Monopolar DES was applied unilaterally to the LC core with biphasic (cathodal leading) square pulses (0.1-0.5 ms, 0.01-0.2 mA). Each LC-DES parameter was repeated 30 times with an interstimulus interval of 4 s. We tested a wide range of single pulse (SP)-DES parameters in order to establish the most effective LC-DES parameters for efficient activity modulation within the entire LC nucleus, while preventing local tissue damage. In our experience, currents exceeding 0.1 mA frequently led to complete loss of LC spiking activity at the dual recording/stimulation electrode. On the basis of our preliminary observations and existing knowledge, the pulse train (TR)-DES conditions were restricted to pulse duration of 0.4 ms, as more efficient for unmyelinated nerve fibers, and current intensity of 0.03 mA and 0.05 mA. We chose a relatively low frequency of LC-DES, taking into account the fact that LC-NE neurons do not naturally express high firing rates. Earlier studies showed that LC stimulation at \sim 20 Hz results in both local (in LC) and distal (in mPFC) NE release (Florin-Lechner et al. 1996; Huang et al. 2007). We aimed to establish the minimal, but effective, LC-DES parameters for detecting changes in mPFC neural activity. Therefore, TR-DES was applied for 50–200 ms at 20-50 Hz.

Monopolar stimulation within the current range used in the present study (<0.2 mA) is estimated to activate cells within a maximal radius that would not exceed 0.5 mm when cell bodies are stimulated (Ranck 1975). None of the stimulation parameters used here elicited jaw or



			Brain	Region		
Linear array channel	Rat 483.5	Rat 484.2	Rat 520.4	Rat 522.1	Rat 535.7	Rat 587.2
ch9	not recorded	not-LC	not-LC - Rec/Stim	not-LC	not recorded	not recorded
ch8	not recorded	not-LC	not recorded	not-LC	not-LC	not-LC
ch10	not recorded	not-LC	not recorded	not-LC	not-LC	not-LC
ch7	not recorded	not-LC	not recorded	not recorded	not-LC	not recorded
ch13	not recorded	not-LC	not recorded	not-LC	not-LC	not-LC
ch4	not recorded	not-LC	not recorded	not-LC	not-LC	LC dorsal border
ch12	not recorded	LC dorsal border	not recorded	not-LC	not-LC	LC - 0.1mm
ch5	not recorded	LC - 0.2mm	not recorded	not-LC	not-LC	LC - Rec/Stim
ch15	LC dorsal border	LC - 0.1mm	not-LC - Rec/Stim	not-LC	not-LC	LC - 0.1mm
ch2	LC - 0.2mm	LC - Rec/Stim	not-LC	LC dorsal border	LC dorsal border	LC - 0.2mm
ch16	LC - 0.1mm	LC - 0.1mm	LC dorsal border	LC - 0.3mm	LC - Rec/Stim	LC - 0.3mm
ch1	LC - Rec/Stim	not-LC	LC - 0.2mm	LC - 0.2mm	not recorded	not recorded
ch14	LC ventral border	not-LC	LC - 0.1mm	LC - 0.1mm	LC - 0.2mm	LC - 0.5mm
ch3	not-LC	LC - 0.4mm	LC - Rec/Stim	LC - Rec/Stim	LC - 0.3mm	LC ventral border
ch11	not recorded	LC ventral border	LC - 0.1mm	LC ventral border	LC - 0.4mm	not-LC
ch6	not-LC	not-LC	LC - 0.2mm	not-LC	LC - 0.5mm	not-LC

Fig. 1. Histological verification and reconstruction of the electrode placement in locus coeruleus (LC) and medial prefrontal cortex (mPFC). *A, left*: coronal view of Nissl-stained section depicting LC core region with the electrode track (arrow) along the medial border of LC (*rat 483.5*). Such electrode placement permitted detection of extracellular LC spikes and effective activation of almost the entire LC nucleus by direct electrical stimulation (DES). Note that the brain tissue in the vicinity of the stimulation electrode is largely intact. Scale bar, 0.1 mm. *Right*: coronal unstained brain section depicting mPFC region and the position of 1 of the 4 shanks highlighted by a fluorescent dye (arrow) of the electrode array used for recording in the mPFC (*rat 457.8*). Scale bar, 0.5 mm. *B* and *C*: reconstruction of all electrode placements in LC (*B*) and mPFC (*C*) from all rats used in the present study (numbers correspond to the rat IDs; in case of bilateral LC recordings the rat ID is indicated twice). Number below each brain section indicates anterior/posterior distance from bregma. Nonfilled and dotted electrode symbols in *B* represent the single electrodes and linear arrays, respectively. Different symbols in *C* are assigned to each rat and represent the tetrode positions where single mPFC units were isolated. *D*: estimated placement of each electrode contact of a linear array within a dorsal-ventral axis in each experiment. Green color highlights the recording sites of the putative LC-norepinephrine (NE) neurons, which were completely inhibited shortly after clonidine injection (0.05 mg/kg ip). Blue color highlights approximate dorsal and ventral LC borders, where spikes from mixed, LC-NE and non-NE, cell populations were recorded; data from the "mixed" recording sites were excluded from analysis. Red color indicates position of the dual recording/stimulation electrode.

facial twitching, which suggests that the effective voltage gradient produced by the stimulation current was likely concentrated around the LC cell bodies and did not spread beyond the LC and activate the nearby adjacent trigeminal pathway. Electrical current was delivered with a biphasic stimulus isolator (BSI-1, Bak Electronics, Mount Airy, MD). The stimulation parameters were digitally controlled by Spike2 software (Cambridge Electronic Design, Cambridge, UK) and transmitted to the current source via a digital-to-analog converter built in to the CED Power 1401mkII data acquisition unit (Cambridge Electronic Design). The voltage passed through the tip of the stimulation electrode was monitored via an in-house custom-designed and built voltage output unit.

The extracellular signals were high-pass filtered (0.1 Hz–8 kHz) with an in-house custom-designed and built preamplifier and amplified (×2k) with an Alpha Omega multichannel processor (MPC Plus, Alpha Omega, Alpharetta, GA). The signals were digitized at 24 kHz with a CED Power1401mkII converter and Spike2 data acquisition software (Cambridge Electronic Design). Power-line noise (50 Hz) was reduced during data acquisition by a high grade of grounding in the electrical infrastructure of the recording room, by grounding every device to a single point, and by keeping the grounding short. The data recorded and analyzed here were minimally affected by line noise contamination.

Identification of LC neurons. The following criteria were used for identification of LC neurons: I) broad spike widths (\sim 0.6 ms), 2) regular low firing rate (1–2 spikes/s), and 3) a brief excitation followed by prolonged inhibition in response to pinch of the contralateral paw (Cedarbaum and Aghajanian 1978). The neurochemical nature of the recorded LC neurons was also verified by injection of clonidine (0.05 mg/kg ip) at the end of each experiment. Clonidine binds to inhibitory α_2 -autoreceptors and results in complete inhibition of LC-NE neurons (Aghajanian and VanderMaelen 1982).

Signal processing. The LFP was extracted from the raw broadband signal recorded in one of the electrodes in mPFC by band-pass filtering between 1 and 250 Hz and downsampling at 500 Hz. The band-limited LFP signals were generated with the following bandwidth settings: delta (1-4 Hz), theta (4-8 Hz), alpha (8-11 Hz), sigma (11-15 Hz), beta (15-20 Hz), Nmod (20-40 Hz), gamma (45–90 Hz). The filtering procedure and selection of frequency bands is described in detail elsewhere (Belitski et al. 2008). The instantaneous band-limited power (BLP) was computed as the square of the absolute value of the Hilbert transform of the band-passed signal of each band (Belitski et al. 2008). To extract the multiunit activity (MUA), the signal was band-pass filtered in the range of 1,000–3,000 Hz and the absolute value of the signal was then taken. The MUA obtained in this way is thought to represent a weighted average of the extracellular spikes of all neurons within a sphere of $\sim 140-300 \mu m$ around the tip of the electrode (Logothetis 2003). To quantify the effect of LC stimulation, the BLP for each frequency range was first normalized to a 1-s prestimulus period (Z score). The evoked BLP response was computed over the entire interstimulus interval of 4 s. The degree of BLP response was estimated as an area under or above the curve of the evoked BLP response. The period for integration was defined from the end of LC stimulation until the BLP signal returned to within ± 1 standard deviation (SD) of the prestimulus values.

For single unit isolation, the signal was first high-pass filtered above 600 Hz and spike shapes exceeding at least twofold the background activity were extracted (Fig. 2) Next, the template matching algorithm complemented by manual cluster analysis based on principal components and on specific waveform measurements was applied with Spike2 software. Both tetrode and single-electrode recordings were submitted to this analysis. The recording was classified as a single unit if a refractory period of at least 1 ms was present between two consecutive spikes (Fig. 2, *B* and *C*). The isolated mPFC single units were further classified into putative pyramidal cells or interneurons on the basis of *I*) the peak-to-trough amplitude ratio, 2) duration of the afterhyperpolarization, and 3) the spontaneous firing

rate. In cases in which the recording technique and spike sorting method did not allow unambiguous single unit isolation, the recording was conservatively classified as MUA. Representative examples of the spike shape overlays for the LC-NE single-unit and multiunit clusters and putative pyramidal mPFC units with their corresponding interspike interval histograms are illustrated in Fig. 2, *B* and *C*.

To characterize the effect of LC-DES on LC spiking activity, peristimulus raster plots and corresponding peri-stimulus time histograms (PSTHs) of the spike density were plotted -0.5 to +1.5 ms around stimulation onset in 20-ms bins. Inspection of PSTHs revealed two major response profiles in LC: inhibition and excitation/inhibition. To classify the LC response type, the LC firing rate was converted to Z scores using 0.5 s of prestimulation period and averaged over all repetitions of the same stimulus parameter. We identified LC inhibition by the presence of at least one 20-ms bin within 100 ms after stimulus onset with a Z score less than -1.96. The excitation/inhibition responses were identified by the presence of the first poststimulus 20-ms bin with a Z score greater than 1.96. The response latency and duration were estimated by the time when the LC firing rate returned to the baseline level.

To characterize the mPFC single-unit responses to LC stimulation, PSTHs were plotted -1.0 to +3.0 s around stimulation onset in 100-ms bins. To normalize the difference in firing rate across neurons, firing rate was converted to Z scores using 1 s before stimulation onset for normalization. Inspection of PSTHs obtained from cortical single units revealed three groups of responses: 1) short-latency inhibition occurring 0-200 ms after stimulation onset (group 1), 2) short-latency excitation occurring 100-300 ms after stimulation onset (group 2), and 3) long-latency and -duration excitation occurring 200-1,000 ms after stimulation (group 3). We then identified group 1 and 2 units as those that had at least one 100-ms bin with a Z score less than -1.96or greater than 1.96, respectively, within a 200-ms window after train stimulation onset. Group 3 units were identified as those that had at least two consecutive time bins with Z > 1.96 between 200 and 1,000 ms after stimulation onset. The proportion of responsive neurons was calculated for each group of mPFC units and for each of the 12 TR stimulation conditions. The two current intensities were eventually combined, yielding the six TR stimulation conditions reported in RESULTS. PSTHs were constructed for all units and for each stimulation condition. Mean and SE of firing rate of the responsive neurons in each group were plotted.

Depth of anesthesia and cortical state. The cortical state in most experiments was highly synchronized (Fig. 2A, top) as reflected by predominant high-amplitude slow wave activity. However, under urethane anesthesia spontaneous transitions to a more desynchronized state are known to occur. It cannot be excluded that, in some instances, the LC-DES itself may affect the global cortical state. Thus, to characterize the cortical state at the time of LC-DES, we computed a cortical synchronization index (SI) by taking the ratio between total delta (1–4 Hz) power and total 1–90 Hz power of the mPFC LFP trace in the 1-s interval preceding stimulation (Curto et al. 2009). In addition, we calculated a cortical activation index (AI) by taking the ratio between total gamma (45–90 Hz) power and total delta (1–4 Hz) power of the mPFC LFP trace. The cortical state indexes (SI and AI) were calculated on a trial-by-trial basis, and the trials in the top and bottom quartiles were selected for further analysis. We repeated the BLP analysis, as described above, for the selection of trials that were characterized by high and low levels of cortical synchronization as reflected by SI. We also compared the responsiveness of mPFC single units (total spike count 500 ms after LC-DES) depending on the overall level of cortical activation by splitting the trials according to the high and low AI calculated over 500 ms after LC stimulation.

Statistical analysis. We used analysis of variance (ANOVA) with a significance level of $\alpha=0.05$ for evaluating the effects of each stimulation parameter (pulse duration, current intensity, stimulation frequency, and duration of stimulation) on LC and mPFC firing and changes in spectral composition of the LFP signal recorded in mPFC.

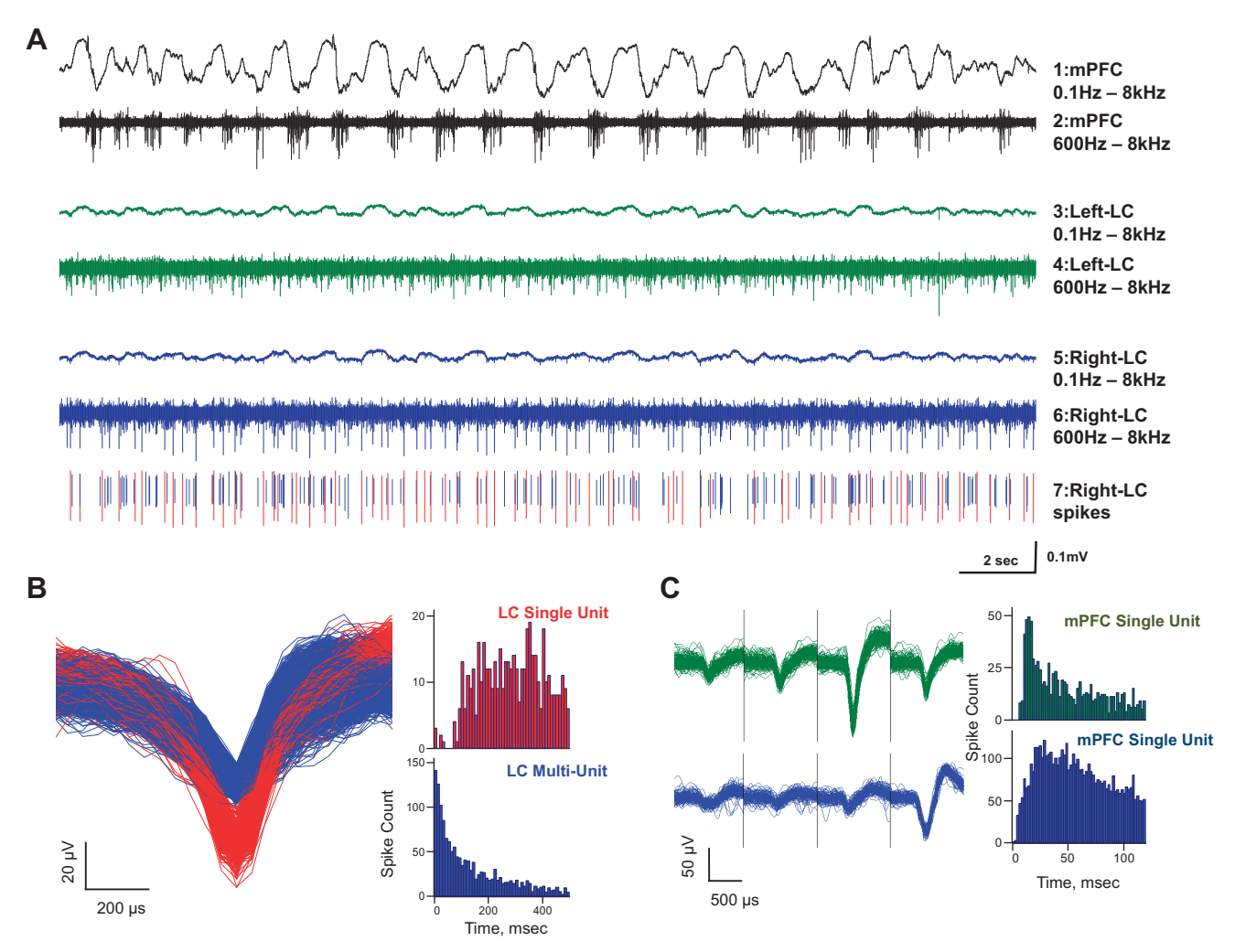


Fig. 2. Simultaneous recording from mPFC and bilateral LC. A: representative traces of simultaneous extracellular recording from the right mPFC (black traces), left LC (green traces), and right LC (blue traces) during spontaneous activity under urethane anesthesia. Note that spontaneous population activity in the mPFC (top) was characterized by high-amplitude slow oscillations indicative for Up and Down states. For each brain region, a wide-band (0.1 Hz–8 kHz) and a high-pass filtered (600 Hz–8 kHz) signal are shown. Trace at bottom shows spike waveforms extracted from the extracellular voltage signal recorded in the right LC. The waveforms could be separated into 2 clusters: the first cluster (red spikes) satisfied a single-unit criterion; the second (blue spikes) was classified as multiunit activity (MUA). B: overlay of the spike waveforms shown in A (bottom) and their corresponding interspike interval histograms. C: overlay of the spike waveforms and their corresponding interspike interval histograms for 2 single units recorded from the same tetrode in the mPFC.

One-sample *t*-test was used for revealing a significant effect of each stimulation parameter on the changes in power for each frequency band.

Perfusion and histology. At the end of the experiment, the rat was euthanized with a lethal dose of pentobarbital sodium (100 mg/kg ip; Narcoren, Merial) and perfused transcardially with 0.9% saline followed by 4% paraformaldehyde in 0.1 M phosphate buffer (PB, pH 7.4). The brain was removed and stored in the same fixative. Before sectioning, whole brains were placed in 0.1 M PB buffer containing 30% sucrose until they sank. Serial 60-\mum-thick coronal sections were then cut on a horizontal freezing microtome (Microm HM 440E, Walldorf, Germany), collected in 0.1 M PB, and then directly stained or stored at -20°C in a cryoprotectant solution (30% ethylene glycol and 10% sucrose in 0.05 M PB) until further processing. Nissl staining was performed according to a standard procedure. Briefly, sections were mounted on gelatin-coated glass slides, defatted, stained with cresyl violet, rinsed with acetic acid, dehydrated, and coverslipped. The placement of silicone-based electrode arrays was visualized by preliminary coating of the back side of the shanks with fluorescent substance (dextran conjugated to Alexa Fluor 546, Invitrogen, Eugene, OR). All sections were examined with an AxioPhot or Axio-Imager microscope (Carl Zeiss, Goettingen, Germany) equipped with

 $\times 2.5$, $\times 5$, $\times 10$, $\times 20$, and $\times 40$ planapochromatic objectives. Nissl sections were examined under bright field. Fluorescent sections were examined under epifluorescent illumination with custom-made sets of filters for Alexa Fluor 546 (AHF, Tuebingen, Germany). A small electrolytic lesion was made by passing constant current between the tip of the stimulating electrode and the ground wire (0.2 mV for 5 s) in order to identify the placement of the electrode tip on histological sections.

RESULTS

We examined the effects of electrical stimulation applied unilaterally to the LC core on spiking activity of putative LC-NE neurons ipsi- and contralateral to the stimulation site. The ipsilateral effects of LC-DES on the firing rate of LC-NE neurons were measured directly at the stimulation site and within dorsal-ventral extension of the LC core with multichannel linear electrode arrays. The mean firing rate of reliably isolated LC single units (25.4% of all isolated spike waveform clusters) was 2.68 \pm 0.32 spikes/s (range: 0.18–7.37 spikes/s). Most of the LC spike waveform clusters (74.6%) did not

satisfy single-unit classification criteria and were conservatively classified as MUA (firing rate range: 1.96–71.6 spikes/s). All multiunit clusters mainly contained spikes of putative LC-NE neurons, as systemic clonidine injection (0.05 mg/kg ip) produced a transient cessation of firing shortly after injection. The recordings with "mixed" MUA (partial inhibition by clonidine) were excluded from analysis. We also characterized the LC-DES-induced modulation of neural activity in the mPFC, an important cortical target of LC, at the level of population activity (LFP) and single units. All LC-DES parameters tested effectively modulated LC neural activity, while only pulse trains produced detectable changes in the neural activity in mPFC.

Histological examination of the brain tissue around the tip of the stimulating electrode confirmed the absence of any substantial current-induced tissue damage, and a large proportion of LC-NE neurons remained intact. Representative histological sections with the electrode tracks in LC and mPFC and reconstruction of the electrode placement for all experiments are illustrated in Fig. 1.

Local effects of LC-DES. We used a dual recording/stimulation electrode for obtaining the extracellular spiking activity of LC at the stimulation site. The custom-built electric switch between the recording and stimulation modes was software controlled such that the stimulation mode was switched on 1 ms before LC-DES and switched off immediately after stimulation offset. As expected, the duration of DES-induced artifact was proportional to the voltage gradient produced by the current passed through the electrode tip. In the case of SP-DES, the recording signal was disturbed for 5–20 ms. The artifact-related signal loss prevented reliable detection of the short-latency LC response. Nevertheless, the most prominent local

effect of LC-DES was a prolonged LC inhibition (Fig. 3A), which exceeded severalfold the pulse duration (0.1–0.5 ms) and lasted from 9 to 470 ms. Furthermore, there was no systematic relationship between SP-DES parameters and duration of LC firing suppression $[F_{1,4} = 0.74, \text{ not significant (ns)}]$ and $F_{1,6} = 1.59$, ns for pulse duration and current intensity, respectively]. Table 1 and Fig. 3B summarize the results obtained for different SP-DES parameters. Currents higher than 0.1 mA often led to complete loss of LC spiking activity at the dual stimulation/recording electrode, resulting in the smaller number of observations (Table 1), which may have compromised the statistical power. However, the overall result remained the same when the data obtained with high currents (0.1 mA and 0.2 mA) were excluded from statistical analysis $[F_{1,4} = 1.21, \text{ ns and } F_{1,6} = 1.61, \text{ ns for pulse duration and } F_{1,4} = 1.21, \text{ ns and } F_{1,6} = 1.61, \text{ ns for pulse duration and } F_{1,6} = 1.6$ current intensity, respectively].

LC-DES consisting of pulse trains (TR-DES) produced a markedly longer LC inhibition, which was proportional to the stimulation strength (Fig. 3, C and D). There was no significant effect of current intensity (0.03 mA vs. 0.05 mA, ns), nor was there a significant interaction between TR-DES parameters; therefore, the data obtained for different currents were combined. Both a higher stimulation frequency (50 Hz vs. 20 Hz; F=33.1, P<0.001) and a longer TR-DES duration (50, 100, or 200 ms; $F_{1,2}=12.7, P<0.001$) produced stronger LC inhibition (Fig. 3D). The average suppression of LC firing greatly exceeded the TR-DES duration and lasted, for example, 285.3 \pm 67.3 ms and 1,252.2 \pm 126.9 ms for the weakest (50 ms at 20 Hz) and the strongest (200 ms at 50 Hz) TR-DES conditions, respectively.

Thus all LC-DES parameters tested in the present study elicited a long-lasting LC inhibition in direct proximity to the

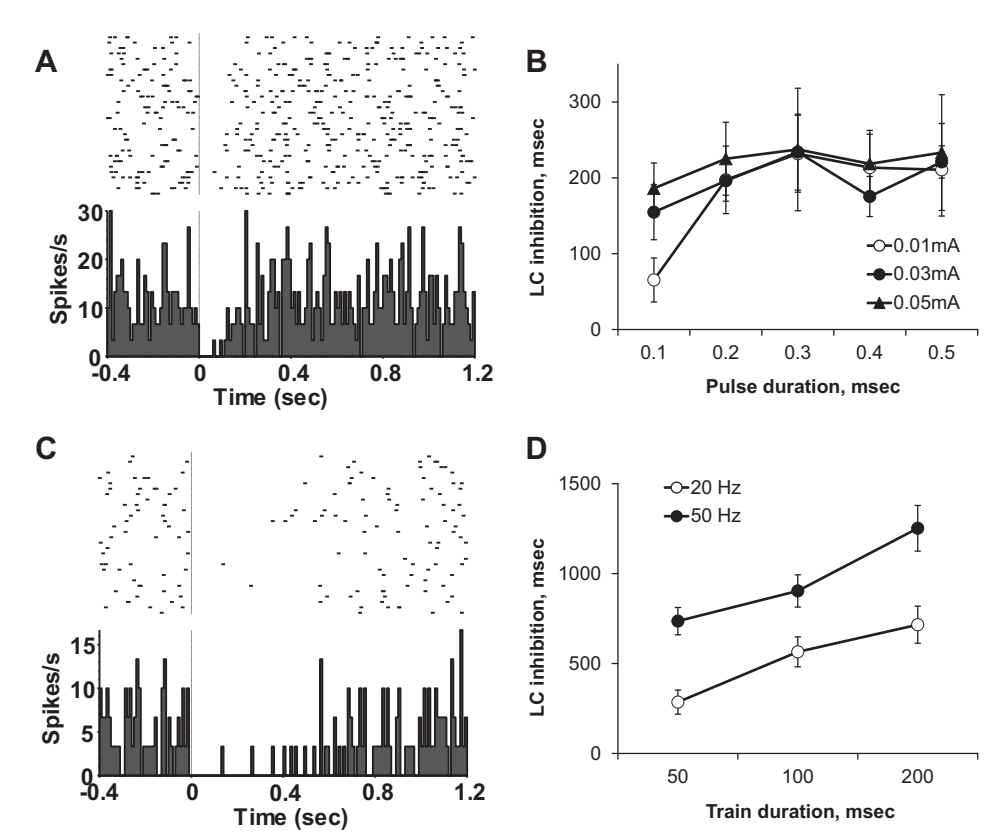


Fig. 3. Sustained suppression of LC neuron firing at the stimulation site. A and C: raster plots and corresponding peristimulus time histograms (PSTHs) show the LC spiking activity around LC-DES onset (t = 0) for 30 repetitions of the same stimulation condition. Two representative examples illustrate a complete cessation of LC firing immediately after application of a depolarizing current. Data plotted in A and C were obtained from the same recording/stimulation site for both single-pulse (SP)-DES (A) and pulse train (TR)-DES (C) conditions. SP-DES: 0.4 ms, 0.05 mA; TR-DES: 6 pulses (0.4 ms, 0.05 mA) at 50 Hz. B and D: dependence of LC inhibition on stimulation strength. Group averages (means ± SE) are plotted for SP-DES (B, n = 10 rats) and TR-DES (D, n = 5 rats). For TR-DES, data from different current intensities (0.03-0.05 mA) were combined. Note that all SP-DES conditions were equally effective, while the duration of LC inhibition was proportional to the number of pulses within a train.

J Neurophysiol • doi:10.1152/jn.00920.2013 • www.jn.org

Table 1.	Duration of	LC inhibition a	and response	probability aft	er a single	pulse stimulation
----------	-------------	-----------------	--------------	-----------------	-------------	-------------------

Current	0.1 ms		0.2 ms		0.3 ms		0.4 ms		0.5 ms	
LC stimulation	n site									
0.01 mA	65.4 ± 29.0	5 (5)	197.4 ± 44.5	7 (7)	231.8 ± 50.7	6 (6)	213.6 ± 44.1	9 (9)	210.7 ± 61.0	6 (6)
0.02 mA	173.2 ± 43.6	6 (6)	175.5 ± 33.5	6 (6)	198.0 ± 36.8	6 (6)	203.5 ± 34.7	6 (6)	217.7 ± 52.2	6 (6)
0.02 mA	173.2 ± 43.0 154.6 ± 36.3	4 (4)	175.3 ± 35.3 196.1 ± 26.9	7 (7)	234.0 ± 50.2	5 (5)	175.4 ± 26.5	9 (9)	217.7 ± 32.2 221.0 ± 21.3	5 (6)
0.05 mA	186.2 ± 33.4	5 (5)	225.3 ± 48.1	8 (8)	237.5 ± 80.8	4 (4)	218.6 ± 44.1	9 (9)	233.4 ± 76.3	5 (5)
0.07 mA	153.0 ± 61.5	4 (4)	176.4 ± 32.1	7 (7)	122.6 ± 45.9	5 (5)	117.6 ± 34.9	7 (7)	160.0 ± 60.1	5 (5)
0.1 mA	128.3 ± 39.0	4 (4)	150.8 ± 58.0	6 (6)	139.3 ± 73.5	4 (4)	158.0 ± 68.7	5 (5)	188.5 ± 78.5	2(2)
0.2 mA	170.7 ± 57.2	3 (3)	66.3 ± 14.3	4 (4)	129.0	1(1)	125.0 ± 75.0	2(2)	168.0	1(1)
LC contralates	ral site									
0.01 mA	n/a	0 (6)	n/a	0(7)	150.0	1 (6)	97.5 ± 24.6	4(7)	146.7 ± 37.1	3 (6)
0.02 mA	100.0	1 (6)	83.3 ± 8.8	3 (6)	105.8 ± 6.8	5 (6)	110.0 ± 5.2	6(6)	103.3 ± 12.0	3 (5)
0.03 mA	105.0 ± 35.2	4 (5)	77.5 ± 21.8	4(7)	90.0 ± 16.1	6(6)	121.8 ± 7.4	5(9)	116.6 ± 7.6	5(5)
0.05 mA	108.2 ± 16.8	5 (6)	117.1 ± 7.1	7(8)	121.7 ± 9.8	6(6)	120.4 ± 8.0	9(9)	125.2 ± 7.9	5(6)
0.07 mA	92.0 ± 14.5	3 (3)	120.2 ± 8.6	6 (6)	101.8 ± 6.4	4 (4)	113.6 ± 9.4	5 (5)	120.7 ± 16.6	3 (3)
0.1 mA	96.7 ± 6.7	3 (3)	128.3 ± 19.9	6 (6)	102.3 ± 15.3	4 (4)	141.2 ± 10.9	5 (5)	197.0 ± 68.5	4 (4)
0.2 mA	123.3 ± 12.0	3 (3)	119.3 ± 10.1	4 (4)	130.0 ± 5.8	3 (3)	122.5 ± 11.8	4 (4)	130.0 ± 0.0	2(2)

Values are means ± SE for direct electrical stimulation (DES) of indicated currents and durations; no. of observations showing inhibition and total no. of cases (in parentheses) are indicated for each stimulation parameter. Note that all single-pulse (SP)-DES parameters effectively elicited locus coeruleus (LC) inhibition at the stimulation site, while overall stronger stimulation parameters (in bold) elicited reliable responses in the contralateral LC. n/a, Not applicable.

stimulation site. The early LC discharge (latency < 5 ms) produced by depolarizing current may have been masked because of signal distortion by stimulation artifact.

Spatial extent of LC-DES: LC responses at distal recording sites. In six experiments, we used 16-channel linear electrode arrays (0.1-mm spacing between the electrode contacts) for multisite recording within the dorsal-ventral extent of the LC nucleus. One electrode of the array served as the dual recording/stimulation electrode, while the remaining 15 channels monitored neural activity dorsal and/or ventral to the stimulation site, with 2-5 recording sites located within the LC nucleus (Fig. 1D). This approach enabled monitoring of the LC firing rate modulation at different distances from the stimulation site. At distal recording sites (0.1–0.4 mm), the LC-DES also produced a prolonged LC inhibition, which in a few cases (6 of 37 total observations) was preceded by a short-latency (~5 ms), brief LC discharge (Fig. 4). The LC excitation/ inhibition response is illustrated in detail in Fig. 4C. In the remaining cases, the fast LC excitation was absent. In a small proportion of observations (23 of 120) LC-DES did not elicit any substantial firing rate modulation at distal (0.2–0.4 mm) recording sites; therefore these cases were excluded from quantitative analysis.

The maximal effect of LC-DES was observed within a radius of ~ 0.1 mm from the stimulation site, with the effect being substantially stronger when pulse trains were applied (Fig. 5A). In contrast to the proximal LC-DES effects, which did not depend on DES parameters (Fig. 3B), the duration of LC inhibition at distal recording sites linearly depended on stimulation strength (Fig. 5, B and C). In the case of SP-DES, both longer pulses ($F_{1,4}$ = 9.0, P < 0.001) and higher currents ($F_{1,3}$ = 14.3, P < 0.001) produced proportionally longer LC inhibition. In the case of TR-DES, the duration of LC inhibition depended on I) distance from the stimulation site (0.1-0.3)mm: $F_{1.3} = 15.7$, P < 0.0001), 2) TR-DES frequency (20 Hz vs. 50 Hz: F = 9.5, P < 0.01), and 3) TR-DES duration $(50-200 \text{ ms: } F_{1.3} = 5.3, P < 0.01)$, while the effect of current intensity (0.03 mA vs. 0.05 mA) did not reach statistical significance (F = 3.5, P = 0.064). There was no significant interaction between any of the factors.

Thus a mild monopolar electrical stimulation delivered to the LC core resulted in a dramatic modulation of the firing rate of LC neurons within a radius ~0.2 mm from the tip of the stimulation electrode. This result indicated that a large proportion of LC neurons were affected by DES, as expected in the rat LC, in which the neurons are tightly packed within a very small volume (~ 0.7 mm anterior-posterior, ~ 0.2 mm mediallateral, ~0.4 mm dorsal-ventral planes; Paxinos and Watson 2005). The LC inhibition was likely mediated by multiple mechanisms including 1) autoinhibition of the LC-NE neurons directly affected by the depolarizing current, 2) inhibition mediated by local NE release from DES-activated LC cells, and 3) antidromic activation of the brain stem inhibitory afferents to LC. Taking into account the LC regulation mechanisms mentioned above, the actual spread of depolarizing current was likely much less than ~0.2-mm radius, and therefore we assume that LC-DES minimally affected the LC neighboring structures.

Contralateral effects of unilateral LC-DES. In the contralateral LC, there was a spiking activity change in 85.0% (n =175) of total SP-DES observations obtained from 11 rats. Typically, the low-intensity currents (0.01–0.03 mA) produced almost exclusively LC inhibition, while the higher-intensity currents (0.05-0.2 mA) also occasionally elicited a biphasic (excitation/inhibition) response (Fig. 6). Overall, the inhibitory response was present in 72.3% of different SP-DES conditions, while biphasic response was more rare (12.6%). The LC inhibition onset latency varied from 10 to 90 ms (28.24 \pm 1.53 ms), and the duration of LC inhibition varied from 10 to 400 ms (116.1 \pm 3.3 ms). Interestingly, neither latency nor duration depended on the SP-DES parameters (latency: $F_{1.4} = 0.28$, ns and $F_{1,6} = 0.32$, ns for current intensity and pulse duration, respectively; duration: $F_{1,4} = 1.77$, ns and $F_{1,6} = 1.96$, ns for current and pulse duration, respectively).

In the TR-DES experiments, similarly to the SP-DES (Fig. 6), the first pulse of the train elicited either inhibition or excitation/inhibition, and the same response pattern would be repeated after subsequent pulses. Overall, the effect magnitude in the contralateral LC was weaker compared with the ipsilateral LC (Fig. 5). Generally, stronger DES parameters were

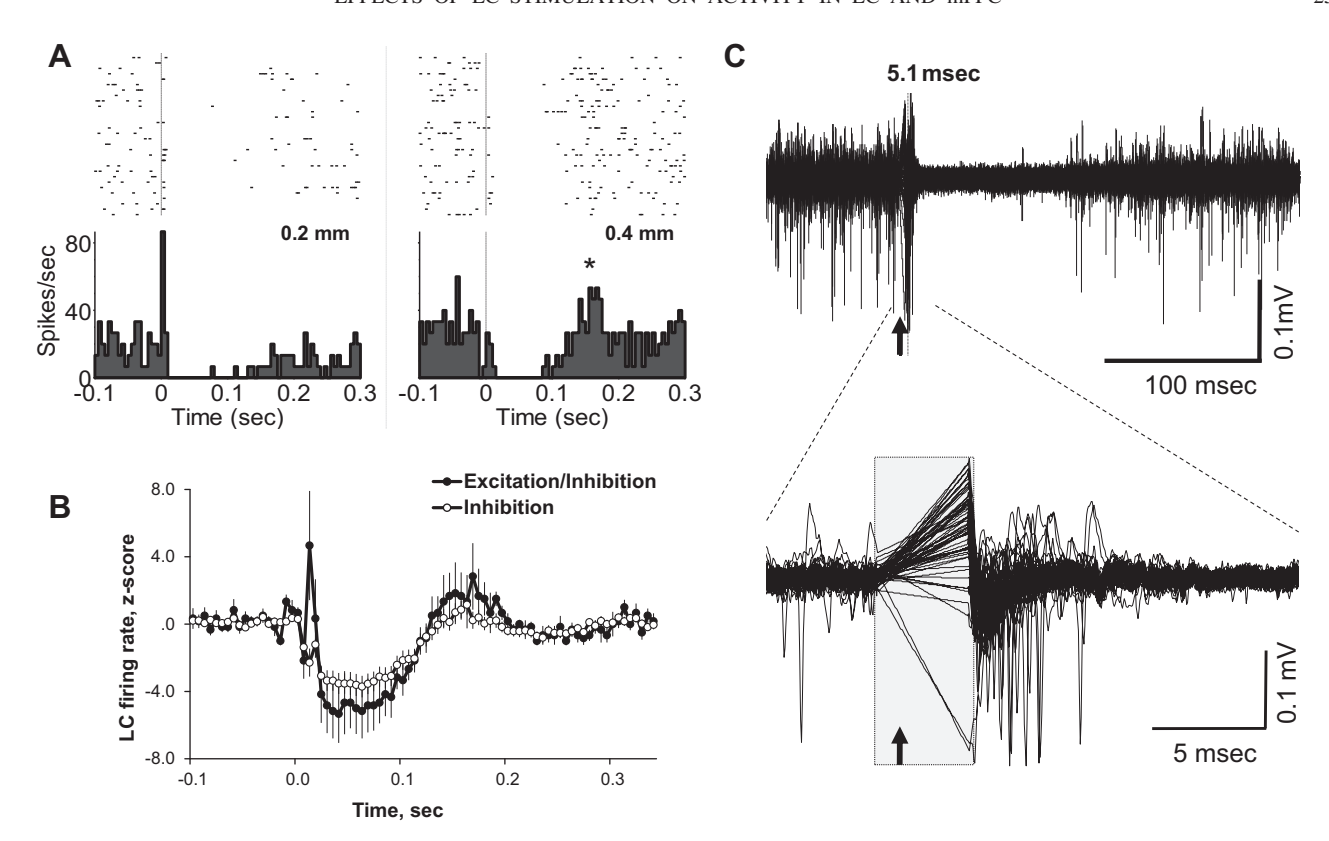


Fig. 4. DES-induced responses in the ipsilateral LC. A: 2 examples of LC neuronal responses to SP-DES (0.2 ms, 0.05 mA). The spikes of LC neurons were simultaneously recorded at 0.2-mm (left) and 0.4-mm (right) linear distance from the stimulation site with a linear electrode array. Raster plots and corresponding PSTHs depict LC firing rate modulation produced by SP-DES over 30 repetitions. A short-latency (\sim 5 ms) burst of firing followed by prolonged inhibition is clearly seen at $top\ left$; this fast LC discharge was not detected at the more distal recording site (0.4 mm, right), while substantial firing inhibition was present. Bin size, 5 ms. Asterisk indicates the rebound excitation. B: averages for all cases showing excitation/inhibition (n = 6 recordings) and inhibition (n = 31 recordings) responses induced by SP-DES in the ipsilateral LC nucleus. Data obtained from all distal recording sites (0.1–0.5 mm from stimulation site) were combined (n = 5 rats). Mean \pm SE normalized firing rate (Z score) is plotted for each response type. C: high-pass (600 Hz–8 kHz) filtered extracellular signal from the example recording shown in A, left, overlaid over 30 trials. Note a short-latency, brief LC discharge followed by long-lasting inhibition; the peak latency of LC burst is indicated. Bottom: the DES-induced LC burst at higher temporal resolution. Gray area indicates artifact-removal period (-1 to 4 ms). Arrows show SP-DES onset.

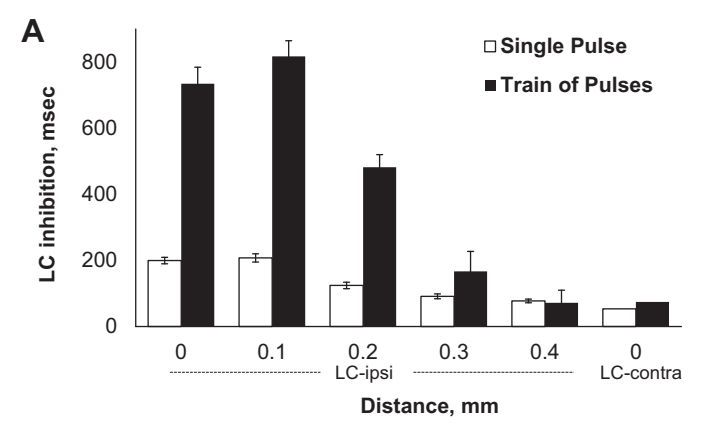
required to elicit reliable responses in the contralateral LC. As indicated in Tables 1 and 2, the proportion of recordings affected by SP-DES increased with longer pulse duration and/or higher current intensity.

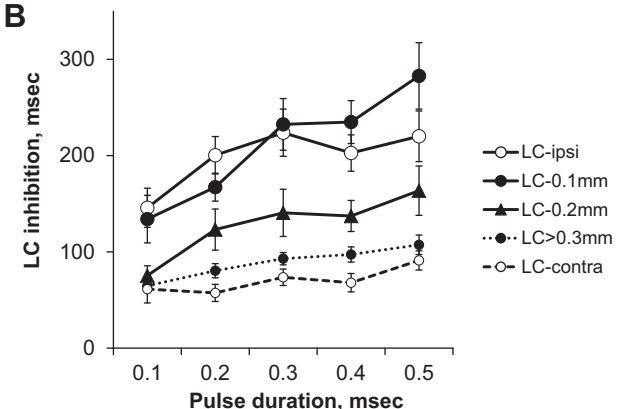
Thus the firing of LC neurons in the contralateral hemisphere was influenced by a putative interplay between the excitatory and/or inhibitory drive generated from the stimulated LC, likely via antidromic activation of bilateral brain stem afferents, and local autoinhibition. The contralateral effects were, however, substantially weaker compared with the ipsilateral side.

Bilateral rebound LC excitation. In addition to DES-induced fast modulation of LC activity (inhibition or excitation/inhibition), we consistently observed a delayed phasic excitation occurring ~ 100 ms after the stimulation offset (Fig. 7, A and B). Strikingly, this rebound LC excitation occurred bilaterally and always followed a DES-induced LC inhibition (Fig. 7, C and D, and Fig. 8). As illustrated in Fig. 8, the delayed LC excitation was observed exclusively at the distal (>0.2 mm) recording sites. Absence of the LC rebound activity at the proximal (0–0.1 mm) recording sites was likely due to strong local LC inhibition. As described above, the inhibition strength gradually declined with distance from the stimulation site, where it could be overcome by LC excitation. Overall, the

rebound activity was more consistently elicited in the contralateral LC; however, it was occasionally observed also at the stimulation site. In the ipsilateral LC, the rebound was present in 40.5% (n=15) of SP-DES tests (n=2 of 5 rats) and in 5.6% (n=25) of TR-DES tests (n=6 of 8 rats). In contrast, in the contralateral LC, the rebound was present in 59.7% (n=123) of SP-DES (n=10 of 11 rats) and in 60% (n=81) of TR-DES recordings (n=7 of 7 rats).

The rebound LC firing rate varied from 62.2% up to 928.0% of the prestimulation baseline rate, and the increase of firing rate during rebound was proportional to the stimulation strength (501.7 \pm 85.4% in case of 200-ms TRs at 50 Hz compared with 226.4 ± 12.2% for all other conditions combined). The rebound peak latency consistently followed the duration of stimulation ($F_{1,2} = 168.4$, P < 0.0001). In case of TR-DES at 20 Hz, the rebound latency was 174.6 ± 6.7 ms, 196.8 ± 5.4 ms, and 292.7 ± 5.2 ms for 50 ms, 100 ms, and 200 ms, respectively. The peak latency was slightly, but significantly (F = 8.9, P = 0.005) shorter for TR-DES at 50 Hz: 163.6 ± 6.8 ms, 191.1 ± 3.7 ms, and 264.0 ± 5.4 ms for 50 ms, 100 ms, and 200 ms, respectively. Remarkably, the delayed rebound LC excitation elicited by TR-DES lasted on average 91.2 \pm 3.5 ms, regardless of pulse frequency (F =0.004, ns) and number of pulses ($F_{1.2} = 0.035$, ns).





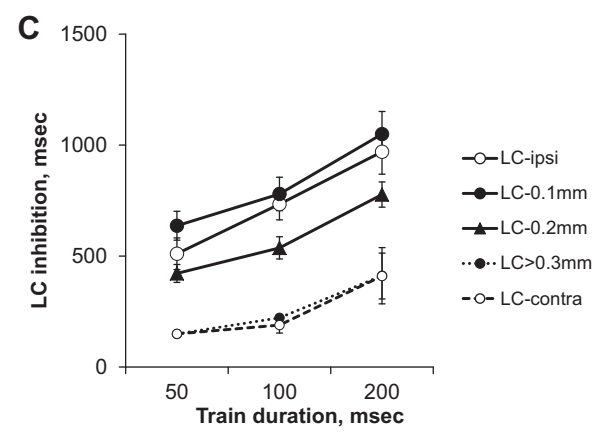


Fig. 5. Duration of LC inhibition ipsi- and contralateral to the stimulation site. A: bars represent average duration of LC inhibition produced by LC-DES at different distances from the stimulation site and in the contralateral LC. Data obtained with identical pulse parameters (0.4 ms, 0.03 mA) are plotted for SP-DES (open bars) and TR-DES (filled bars). Note a gradual decrease of LC inhibition with distance from the stimulation site and substantially weaker inhibition in the contralateral LC. B and C: duration of LC inhibition for different SP-DES (B) and TR-DES (C) conditions. The averages from all current intensities are plotted. LC-ipsi, recordings obtained at stimulation site with a dual recording/stimulation electrode; LC-0.1 mm, recordings obtained 0.1 mm from the stimulation site with a linear array; LC-0.2 mm, recordings 0.2 mm from the stimulation site; LC>0.3 mm, recordings 0.3–0.5 mm from the stimulation site; LC>contra, recordings from the contralateral LC.

In summary, our results demonstrate that DES applied unilaterally to the LC core elicits fast inhibitory or biphasic (excitation/inhibition) responses in both LC nuclei. Unexpectedly, the unilateral LC-DES produced a delayed synchronous excitation of both LC nuclei occurring ~ 100 ms after stimulation offset. Most importantly, the LC firing pattern induced

by DES resembled a characteristic response of LC-NE neurons to a strong excitatory input.

Effects of LC-DES on mPFC population activity. After the detailed characterization of DES-induced responses in LC, we examined the effect of LC-DES on mPFC neural activity ipsilateral to the LC stimulation site. We first focused on the frequency modulation in the LFP signal as indication of a potential change in synaptic input and intracortical processing (Logothetis 2003). Under urethane anesthesia, cortical LFPs are characterized by regular high-amplitude fluctuations with dominant frequency of ~ 1 Hz (Fig. 2A, top) that reflect synchronous transitions of a large population of cortical neurons from Up (active) to Down (silent) states, often referred to as a "synchronized" cortical state (Clement et al. 2008; Curto et al. 2009; Steriade et al. 1993). We restricted analysis to the periods of synchronized cortical state, as this state was predominant in our experiments. The average prestimulation amplitude of the filtered (1–4 Hz) and rectified signal was $0.17 \pm$ 0.01 mV and did not significantly differ between different LC-DES conditions. None of the SP-DESs affected the cortical LFP signal at any frequency range (data not shown). In contrast, TR-DES systematically produced transient (~1 s) periods of cortical activation, or "desynchronization" reflected in the low-amplitude, high-frequency LFP signal (Fig. 9A). Therefore, only the data from TR-DES were quantitatively analyzed.

To quantify the above observation, we used a BLP analysis (Belitski et al. 2008). For each of the eight predefined frequency bands, the integral index of the evoked BLP response was subjected to statistical analysis (see METHODS for details). Figure 9B illustrates an example of LC-DES-induced BLP modulation in the mPFC. There was a significant effect of frequency band ($F_{1.7} = 12.8$, P < 0.001), indicating that the degree of signal power change varied across bands. Overall, the LC-DES caused a significant decrease at low frequencies (1-4 Hz and 4-8 Hz; 1-sample t-test, P < 0.01) and a significant increase in all bands above 20 Hz, including MUA (Fig. 9C). Typically, a stronger LC-DES elicited a stronger change in cortical state as reflected by both the magnitude of BLP change and the frequency ranges affected by LC-DES. Overall, the most consistent effect of LC-DES was observed for frequency ranges above 20 Hz, including MUA. The power modulation of lower frequencies was less consistent across TR-DES conditions, possibly because of spontaneous fluctuations of the depth of urethane anesthesia. For example, during prestimulation periods characterized by the highest delta wave amplitudes (>0.3 mV), the standard LC-DES failed to elicit cortical desynchronization, unless longer pulse trains and/or higher pulse frequencies were used (e.g., 500- to 1,000-ms trains of pulses at 100 Hz; data not shown).

To specifically address a question about the state-dependent effects of LC-DES, we calculated the cortical synchronization index (SI) by taking the ratio between total delta (1–4 Hz) power and total 1–90 Hz power of the mPFC LFP trace in the 1-s interval preceding LC-DES (Curto et al. 2009). The high and low SIs label the trials with high and low levels of cortical synchronization, respectively. We next split all TR-DES trials into three subgroups according to SI index and calculated the power for each band 1 s before and 1 s after LC-DES. The results are summarized in Table 3 and Fig. 9E. Overall, the DES-induced BLP modulation was detected for all groups of trials

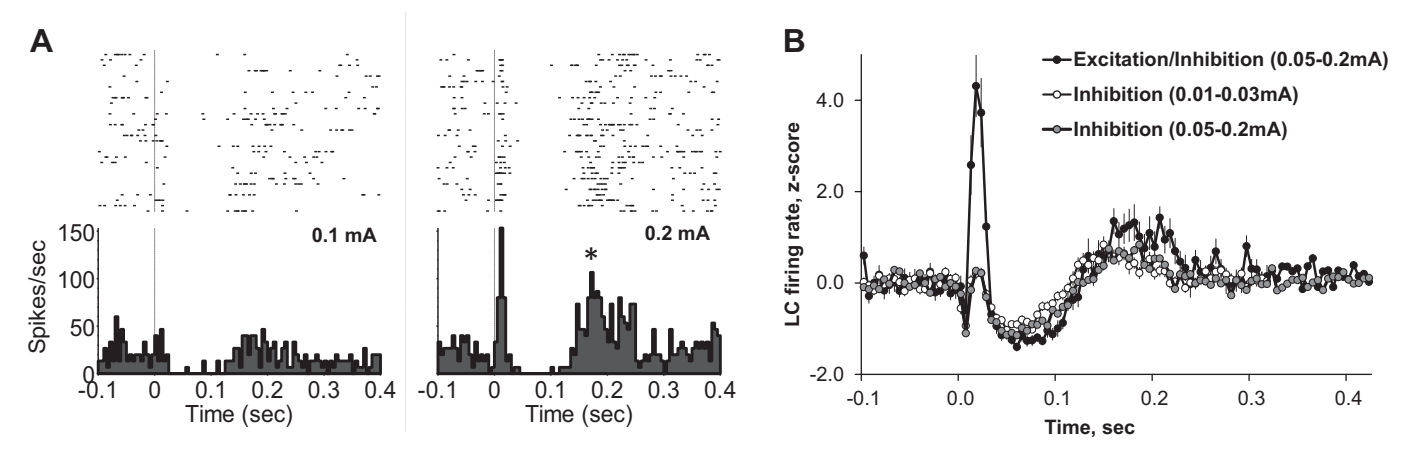


Fig. 6. LC-DES-induced effects in the contralateral LC. A: raster plots and corresponding PSTHs show responses elicited in the contralateral LC by SP-DES of different current intensities: 0.4 ms, 0.1 mA (left) and 0.4 ms, 0.2 mA (right). A short-latency (\sim 10 ms) burst of firing followed by prolonged inhibition is clearly seen at *top right*, while no burst firing preceded LC inhibition in case of weaker current (left). Asterisk indicates the rebound excitation. B: LC spiking activity around LC-DES onset showing inhibition or excitation/inhibition responses in the contralateral LC. The average (mean \pm SE) normalized firing rate (Z score) is plotted for each response type. Low current range: 0.01–0.03 mA (n = 47); high current range: 0.05–0.2 mA (inhibition: n = 53; excitation/inhibition: n = 23). Note that a short-latency LC discharge was elicited exclusively by higher-intensity currents.

and all frequency bands. Moreover, as described above, the tendency for decreased power in the lower frequency range (1-20 Hz) and increased power in the high frequency range (>20 Hz) was present in all types of trials. The most prominent power decrease was observed for delta (1-4 Hz) band in a subset of trials with a highly synchronized cortical state (Fig. 9E). Not surprisingly, there were no dramatic changes in the delta range during the "desynchronized" cortical state, which is characterized by low delta power. Importantly, LC-DES resulted in gamma (45-90 Hz) power increase independent of the cortical state (Fig. 9E).

Finally, we tested whether the observed effects were mediated by NE release associated with LC discharge. In a subset of rats (n = 5), we compared the LFP responses to TR-DES before and after systemic administration of clonidine (0.05 mg/kg ip), an agonist of α_2 -adrenergic receptors. This dose of clonidine suppresses (~50% baseline) LC spontaneous firing for at least 1 h after injection (unpublished observations) and reduces presynaptic NE release through a negative feedback mechanism (Langer 1980). The data sets from TR-DES parameters that elicited reliable cortical desynchronization during baseline were included for analysis. LC-DES applied after clonidine injection was substantially less efficient in changing the cortical state, as reflected by significantly weaker BLP modulation for most of the frequency bands (paired t-test, P <0.05 comparing BLP changes before and after clonidine injection), except for sigma (11-15 Hz) and Nmod (20-40 Hz) bands (paired *t*-test, ns). Moreover, in the presence of clonidine the LC-DES did not elicit a significant power change in any of the frequency bands (Fig. 9D). This result indicates that NE release in the LC subcortical and cortical targets critically contributes to cortical desynchronization.

Effects of LC phasic activation on mPFC single-unit activity. We also analyzed the effects of LC-DES on the firing rate modulation of mPFC single units. Consistent with previous studies, SP-DES did not affect the firing rate of cortical neurons (Dillier et al. 1978; Mantz et al. 1988; Phillis and Kostopoulos 1977). We found, however, that TR-DES produced three major response types (Fig. 10). Prior to their description, we note here that the changes in mPFC firing rate after LC-DES did not differ significantly between the two current intensities we tested (0.03 mA and 0.05 mA); therefore, we combined the data from both intensities for further analysis. Also, the preliminary analysis of mPFC responses within each cortical layer and mPFC subregion did not allow us to draw any convincing conclusions, and we therefore combined single units across all layers and subregions of mPFC (Fig. 1C). The number of isolated single units for each of the six TR-DES conditions is indicated in Table 4. Group 1 units were transiently inhibited, while group 2 and group 3 units were transiently excited after TR-DES (Fig. 10A). It is important to note the jitter in the latency of increased spiking on each trial and the lack of response on some trials (Fig. 10A, left, raster plots), which both indicate that the short-latency activation of group 2 units was not merely antidromic activation of mPFC afferents to the LC (Branchereau et al. 1996). Regardless of the different response profiles, all mPFC single units included for analysis could be classified as putative pyramidal neurons on the basis of their spike waveform characteristics and spontaneous firing rate. The average peak-to-trough duration was 0.680 ± 0.005 ms, peak-to-trough ratio was 3.24 ± 0.04 , and duration of afterhyperpolarization was 1.103 ± 0.007 ms. None of the above features differed across groups 1, 2, and 3. The group 1 neurons had a slightly higher firing rate of 3.24 ± 0.26 Hz

Table 2. Number and proportion of response types in contralateral LC

	0.01 mA	0.02 mA	0.03 mA	0.05 mA	0.07 mA	0.1 mA	0.2 mA
Inhibition Excitation/inhibition	6 (18.9) 1 (3.1)	14 (50.0) 2 (7.1)	23 (71.9) 1 (3.1)	28 (80.0) 4 (11.4)	14 (73.7) 5 (26.3)	15 (68.2) 7 (31.8)	6 (35.3) 10 (58.8)
Unchanged	25 (78.1)	12 (42.9)	8 (25.0)	3 (8.6)	0 (0)	0 (0)	1 (5.9)

Values are number and proportion (in parentheses) of response types for indicated DES currents.

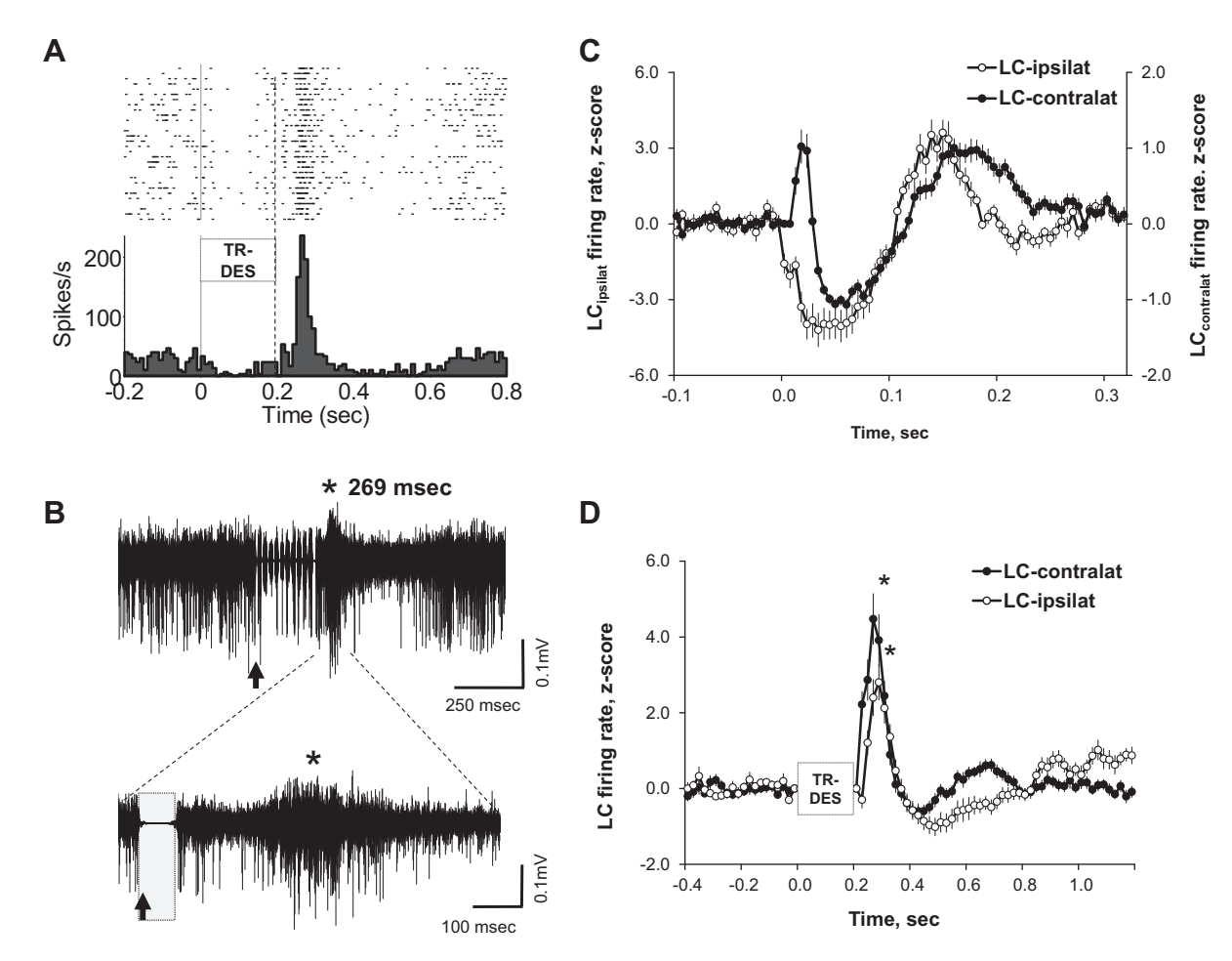


Fig. 7. DES-induced rebound phasic excitation in the contralateral LC. A: raster plot and PSTH depicting the firing rate modulation in the contralateral LC after application of TR-DES (pulse: $0.4 \, \text{ms}$, $0.05 \, \text{mA}$ at $50 \, \text{Hz}$ for $200 \, \text{ms}$). Note a robust poststimulation (\sim 270 ms) burst of firing. Vertical lines indicate stimulation on- and offset. B: high-pass ($600 \, \text{Hz}-8 \, \text{kHz}$) filtered raw signal of the same recording as illustrated on A overlaid over $30 \, \text{trials}$. Increased spike density is observed after TR-DES offset. The peak latency of the rebound LC excitation is indicated. The same recording episode is shown at higher temporal resolution at *bottom*. Gray bar indicates the artifact-removal period ($-1 \, \text{ms}$ to $5 \, \text{ms}$) around the last pulse of the train. Arrows indicate TR-DES onset. $C \, \text{and} \, D$: group averages of all cases with rebound LC excitation ipsilateral and contralateral to the stimulation site after SP-DES (C) and TR-DES (D). Mean \pm SE of the normalized firing rate ($Z \, \text{score}$) is plotted around LC-DES onset. Asterisks show rebound excitation.

compared with 1.28 \pm 0.09 Hz and 1.66 \pm 0.12 Hz for *group* 2 and *group* 3 neurons, respectively.

We next compared the temporal dynamic of the firing rate modulation between different groups of mPFC units. A plot of the time course of firing rate change for all of the single units (n = 291) recorded with the most effective LC-DES (200 ms at 50 Hz) illustrates the three responsive groups of units as well as the remaining units (group 4) that did not meet significant response criteria (Fig. 10B). The group mean data obtained using the same LC-DES parameters for each group of units are plotted in Fig. 10C. Group 1 units were inhibited shortly (within \sim 100 ms) after the LC-DES onset, and this inhibition lasted for the entire duration of LC stimulation (t = 200 ms) (Fig. 10C). Group 2 units increased firing probability starting 100 ms after LC-DES onset, and the excitation lasted for at least 100 ms after the end of LC-DES (t = 300 ms) (Fig. 10C). Group 3 units were characterized by delayed excitation that began after LC-DES (t > 200 ms) (Fig. 10C). Interestingly, firing rate remained elevated until t = 700 ms, which is 500 ms after the last stimulation pulse. Notably, the time course of increased firing rate of group 3 units corresponded to the

duration of LFP power change and increased MUA activity (Fig. 9, A and B).

Further analysis revealed a systematic relationship between the LC stimulation strength (duration and frequency) and the degree to which mPFC single-unit firing rate was modulated. The two following observations support this result. First, the number of significantly modulated units increased with increasing stimulation duration and frequency (Table 4). For instance, 74% of units remained nonmodulated by the weakest stimulation condition (50 ms at 20 Hz) whereas only 52% of units were nonmodulated in the strongest stimulation condition (200 ms at 50 Hz). Second, the magnitude of firing rate modulation was related to stimulation duration in all three groups of responsive units (Fig. 11). For each group of responsive units, the plots in Fig. 11 illustrate the mean change (Z score) in firing rate across the population of responsive units. ANOVA (with 100-ms time bins as a repeated measure) revealed a significant interaction (P < 0.0001 for all comparisons) between LC-DES duration (50-200 ms) and time bin in each group of units (with only exception for group 1 units, 20 Hz TR-DES, Fig. 11, top left). Accordingly, longer duration of

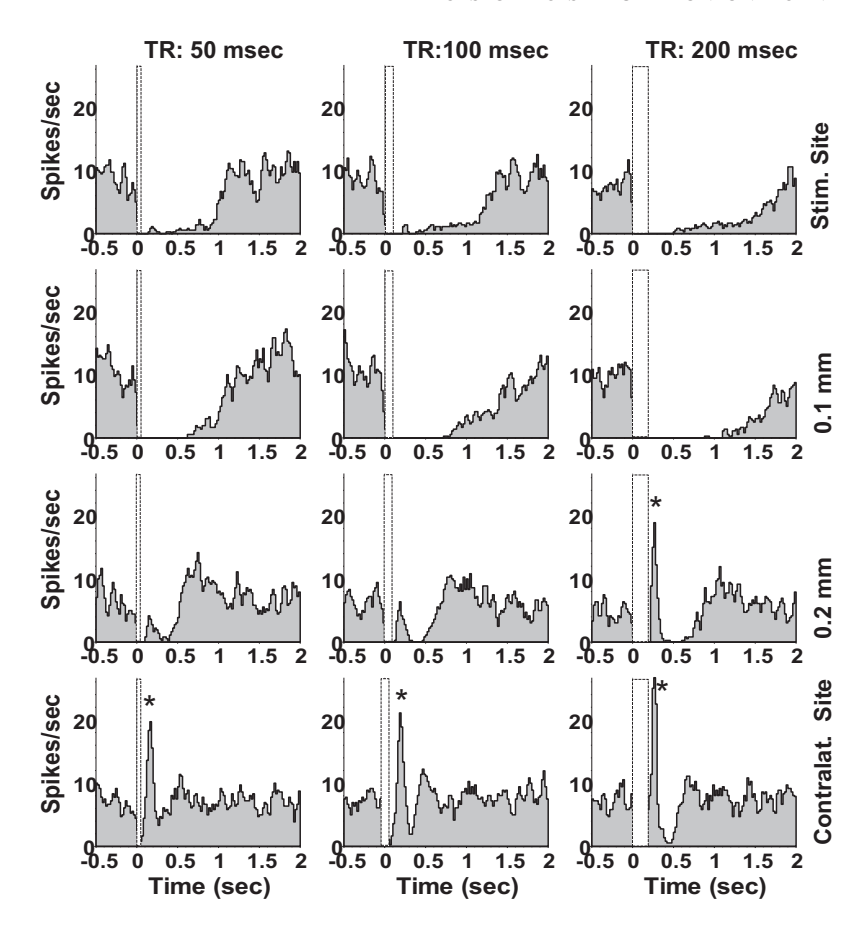


Fig. 8. Modulation of LC firing rate produced by TR-DES at different recording sites: an exceptional example of multisite recording within LC using linear electrode arrays obtained simultaneously with recording in the contralateral LC. LC responses to TR-DES (0.4 ms, 0.05 mA at 50 Hz) are shown for different TR-DES durations. Bin size = 20 ms with boxcar smoothing. Note a robust rebound LC excitation (indicated by asterisks) at the distal recording site (0.2 mm) and in the contralateral LC.

LC-DES was associated with greater mPFC inhibition (*group 1* units, Fig. 11A, *right*) and greater mPFC excitation (*group 2* and 3 units, Fig. 11, B and C).

Finally, we took advantage of the simultaneous recording of the population (LFPs) and single-unit activity in mPFC and correlated the overall magnitude of the cortical activation produced by LC-DES with responsiveness of mPFC single units. To this end, we calculated a cortical activation index (AI) by taking the ratio between total gamma (45–90 Hz) power and total delta (1-4 Hz) power of the mPFC LFP trace. High and low AIs label the trials characterized by high and low levels of LC-DES-induced cortical activation, respectively. We then selected the trials with the top and bottom quartiles of AI calculated over 500 ms after LC-DES and calculated the total spike count over the same time interval for each mPFC single unit in those selected trials. Cortical population activation (or desynchronization) was associated with greater responsiveness of single units to LC-DES in that DES-induced inhibition was stronger and DES-induced excitation was also stronger during trials with higher level of cortical activation as reflected by AI (Fig. 10D). In the case of group 1 units, greater cortical activation produced by LC-DES was associated with stronger firing inhibition compared with the trials when LC-DES was less effective ($t_{303} = -4.04$, P < 0.0001). Similarly, in the case of group 3 units, greater cortical activation was associated with higher responsiveness at the single-unit level as estimated by the higher number of elicited spikes ($t_{696} = 4.96$, P <0.0001). Interestingly, the spike count of group 4 units (nonmodulated) also significantly correlated with the level of cortical population activation produced by LC-DES ($t_{267} = 4.0$,

P < 0.0001). Although "nonresponsive" units did not have a significant modulation of trial-averaged post-DES firing rate (*group 4*, Fig. 10*B*), these neurons emitted more spikes during the subset of trials with a higher level of cortical activation. The spike count of *group 2* units (fast excitation) did not depend on the cortical state ($t_{479} = 0.05$, ns).

Overall, our data demonstrate that LC phasic activation modulated mPFC ongoing activity at both single-unit and population levels. There was a systematic relationship between the LC stimulation strength and the magnitude of mPFC activity modulation. Specifically, the stronger LC stimulation affected firing rate of a larger number of mPFC single units, produced stronger modulation of single-unit firing, and reliably induced changes in cortical population activity. Clearly, a brief, mild electrical stimulation of the brain stem LC nucleus resulted in relatively quick (~100 ms) and sustained (~1 s) modulation of the mPFC activity.

Specificity of LC-DES. An important issue in any such study is the specificity of DES, namely, the degree to which electrical stimulation predominantly reflected activation of LC neurons rather than concurrent activation of neighboring neuronal populations. We have examined this in a number of control experiments. First, analysis of distal LC recording sites indicated that the spread of the depolarizing current was minimal (<0.2 mm). Therefore, stimulation of cell bodies and axons in neighboring structures is unlikely. Equally unlikely is the excitation of fibers of passage; however, such a possibility cannot be completely excluded.

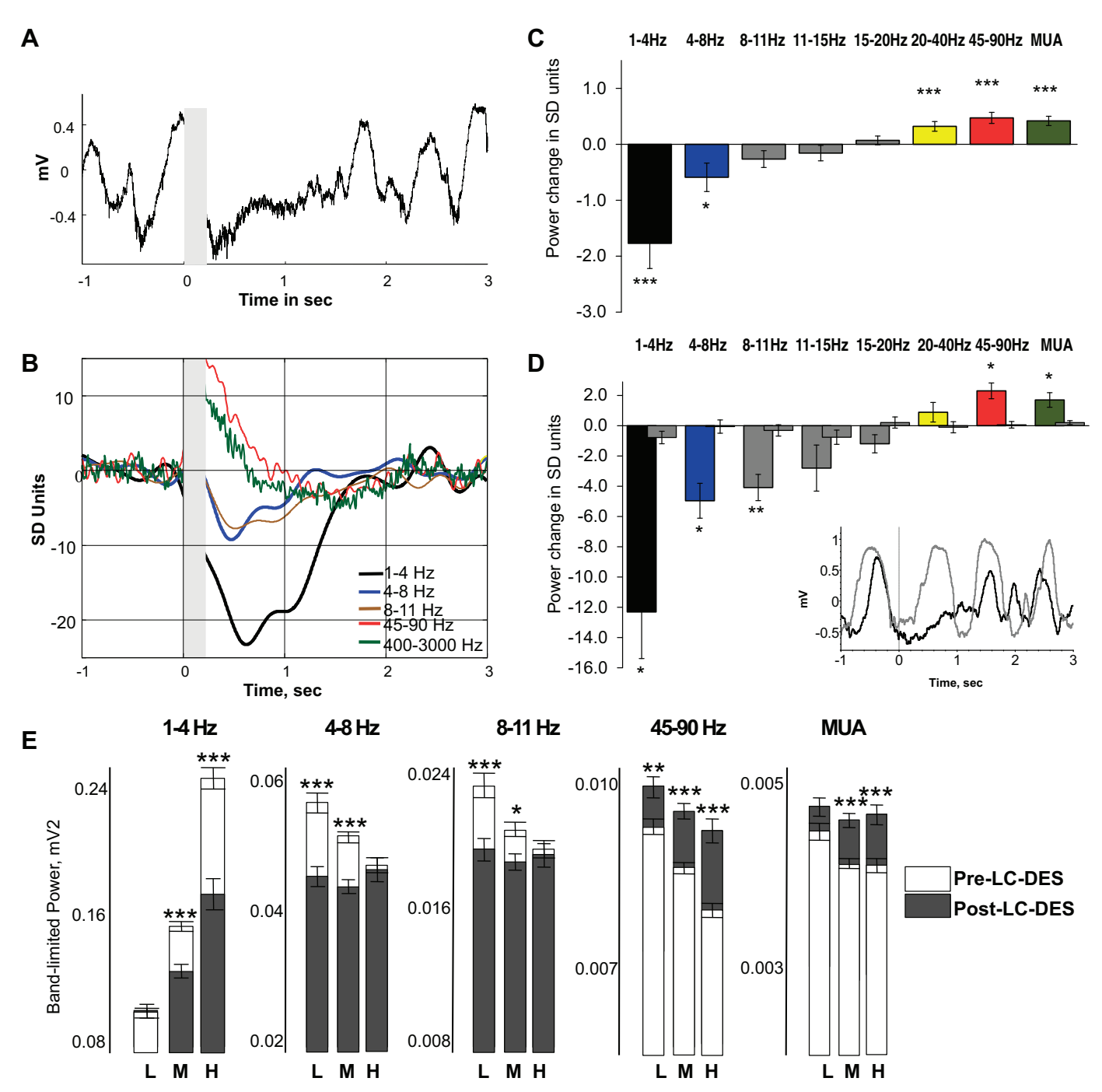


Fig. 9. LC-DES-induced transient cortical activation. A: mPFC wide-band (0.1 Hz-8 kHz) recording depicting a brief (\sim 1 s) cortical activation or desynchronization caused by LC-DES (0.4 ms, 0.05 mA pulses at 50 Hz for 200 ms). B: example of the band-limited power (BLP) modulation produced by the same LC-DES as shown in A. The average BLP change over 30 trials is plotted. Gray bars in A and B indicate stimulation period. C and D: bars represent average values (means \pm SE) of the integral index of the BLP changes produced by LC-DES in all rats tested with TR-DES (n=6; C) and in a subset of rats that received clonidine injection (n=5; D) before (left) and after (right) clonidine injection. Data from all TR-DES conditions were combined, but a subset of stronger TR-DES parameters was tested under clonidine. *P < 0.05, *P < 0.01, *P < 0.001 (1-sample t-test). Inset in D shows 2 representative local field potential (LFP) traces before (black) and after (gray) clonidine injection. Note a more pronounced slow activity after clonidine injection and absence of transient desynchronization after LC-DES. E: cortical state-dependent effects of LC-DES. Bars represent the absolute values (means \pm SE) of BLP 1 s before and 1 s after LC-DES. Trials were sorted with the cortical synchronization index (SI): L group, trials with the lowest SI values (bottom quartile; low level of cortical synchronization, or "desynchronized" state); H group, trials with the highest SI values (top quartile; a highly "synchronized" cortical state); M group, trials with intermediate SI values. Note that signal power in delta (1–4 Hz) band significantly decreased after LC stimulation in M and H groups but not when LC-DES was presented during desynchronized state (L group). Importantly, the DES-induced increase in gamma (45–90 Hz) power was significant for all groups of trials. *P < 0.05, *P < 0.01, *P < 0.01, *P < 0.001 (paired t-test comparing BLP before and after LC-DES).

Table 3. Cortical state-dependent BLP responses to LC-DES

	L Trials	M Trials	H Trials	
Delta (1–4 Hz) Theta (4–8 Hz) Alpha (8–11 Hz) Sigma (11–15 Hz) Beta (15–20 Hz)	\	*** *** * ***	\ ***	
Nmod (20–40 Hz) Gamma (60–90 Hz) MUA (1,000–3,000 Hz)	^ **	^ *** ^ *** ^ ***	^ *** ^ *** ^ ***	

BLP, band-limited power; L trials, trials with lowest synchronization index (SI) values; M trials, trials with intermediate SI values; H trials, trials with highest SI values; MUA, multiunit activity. *P < 0.05, **P < 0.01, ***P < 0.001 (paired *t*-test).

Second, in one experiment using the linear electrode array, we deliberately used the stimulating electrode contacts placed either in cerebellum or in the subcoeruleus region as control stimulation sites. In two additional experiments conducted under failure to target the LC, the placement of the stimulating electrode was 0.2 mm posterior to the LC core, in the medial vestibular nucleus, and 0.3 mm medial in the posterior dorsal tegmental nucleus. In all such cases of control stimulation (in cerebellum, subcoeruleus, medial vestibular nucleus, or posterior dorsal tegmental nucleus), we did not observe any detectable changes in the mPFC neural activity (data not shown).

DISCUSSION

In the present study we examined the effects of unilateral phasic LC activation by means of DES 1) on the firing rate of LC neurons and 2) on the ongoing neural activity in the mPFC, a prominent cortical target of LC that is most relevant for variety of cognitive functions. Although DES is a widely employed technique in neurophysiology and medicine, the current-induced effects on the neural elements being stimulated, as well as on their targets, remain poorly understood (Borchers et al. 2012; Logothetis et al. 2010). The most consistent effect of LC-DES was sustained LC inhibition, which in some cases was preceded by a short-latency burst of firing and/or was followed by a delayed rebound LC excitation. The effects of LC-DES in the mPFC included a cortical state shift and bidirectional modulation of the firing rate in various populations of mPFC neurons. Importantly, the LC firing pattern produced by DES resembled the naturalistic response of LC-NE neurons to salient stimuli (Bouret and Richmond 2009; Bouret and Sara 2004; Chen and Sara 2007; Foote et al. 1980). The latter observation makes DES a valuable experimental tool for investigating the role of phasic LC activation for behavior and cognition and the corresponding underlying neurophysiological mechanisms.

Response patterns elicited by DES in LC neurons. The most prevalent effect of LC-DES was a prolonged suppression of LC firing with inhibition onset latency of ~10–30 ms. In some experimental conditions, the LC inhibition was preceded by a brief neuronal discharge. Both response profiles (inhibition and excitation/inhibition) were observed bilaterally; however, the DES effects were weaker in the contralateral LC. Our data are in agreement with a long-standing notion that the LC spike-dependent mechanism substantially contributes to the LC sustained inhibition via local NE release from the activated

LC-NE neurons and activation of α_2 -adrenoreceptors (Aghajanian and VanderMaelen 1982; Ennis and Aston-Jones 1986). In addition to autoinhibition, some LC-NE neurons, which were not directly excited by the depolarizing current, could be inhibited via volume NE release from the LC neurons that were affected by DES. The local LC inhibition could be also elicited by subthreshold stimulus intensities (Aghajanian et al. 1977; Ennis and Aston-Jones 1986; Watabe and Satoh 1979). Finally, antidromic activation of LC inhibitory brain stem afferents, the nucleus paragigantocellularis (PGi) and the nucleus prepositus hypoglossi (PrH), and GABAergic neurons in the peri-LC dendritic zone (Aston-Jones et al. 1991b, 2004; Ennis and Aston-Jones 1989) may have also contributed to suppression of LC firing. The PGi provides both excitatory and inhibitory input to LC, and the PrH provides inhibitory input (Aston-Jones et al. 1986, 1991b; Ennis et al. 1992). Therefore, we assume that, overall, the firing rate of a substantial population of LC neurons was modulated either directly by the depolarizing current or indirectly via local mechanisms regulating LC activity.

A slightly different mechanism may have mediated responses in the contralateral LC. There is no known monosynaptic connection between the two LC nuclei (Aston-Jones et al. 1991b; Luppi et al. 1995). Therefore, the evoked response in the contralateral LC was a result of interplay between the excitatory and inhibitory contralateral LC afferents and local autoinhibition. It is also possible that unilateral LC-DES antidromically activated the contralateral axons of the LC afferents, PGi and/or PrH. Regardless of a particular response profile and underlying mechanisms, the duration of LC inhibition was proportional to the stimulation strength and inversely related to the distance from the stimulation site. Taking into account these results, we suggest that the duration of LC inhibition may, in principle, serve as a quantitative measure of the amount and spread of NE released by LC-NE neurons affected by DES.

The most striking and rather unanticipated finding of the present study was a rebound LC activation that occurred bilaterally ~100 ms after stimulation offset. The rebound phasic LC excitation was present in the contralateral and distal (>0.2 mm) ipsilateral LC recording sites. The rebound peak latency linearly depended on the DES parameters, while the duration of rebound activity (~90 ms) was similar in all conditions. Typically, the rebound LC excitation was preceded by LC firing suppression and, in turn, could be followed by another period of LC inhibition. To our knowledge, the bilateral LC phasic excitation produced by unilateral LC-DES was experimentally demonstrated for the first time. This new observation is extremely valuable for the interpretation of existing and future studies employing unilateral LC stimulation. Specifically, this result indicated that unilateral LC activation will, most likely, result in substantial NE release in the contralateral forebrain targets of LC.

LC phasic activation rapidly modulates mPFC activity. The LC phasic activation by DES resulted in a rapid change of neural activity in the ipsilateral mPFC. First, we confirmed earlier observations that only trains of pulses were efficient in eliciting changes in cortical activity (Mantz et al. 1988; Olpe et al. 1980; Phillis and Kostopoulos 1977). Our results showed that SP-DES delivered to the LC core with a weak current (0.01 mA) was sufficient to affect firing of the local LC

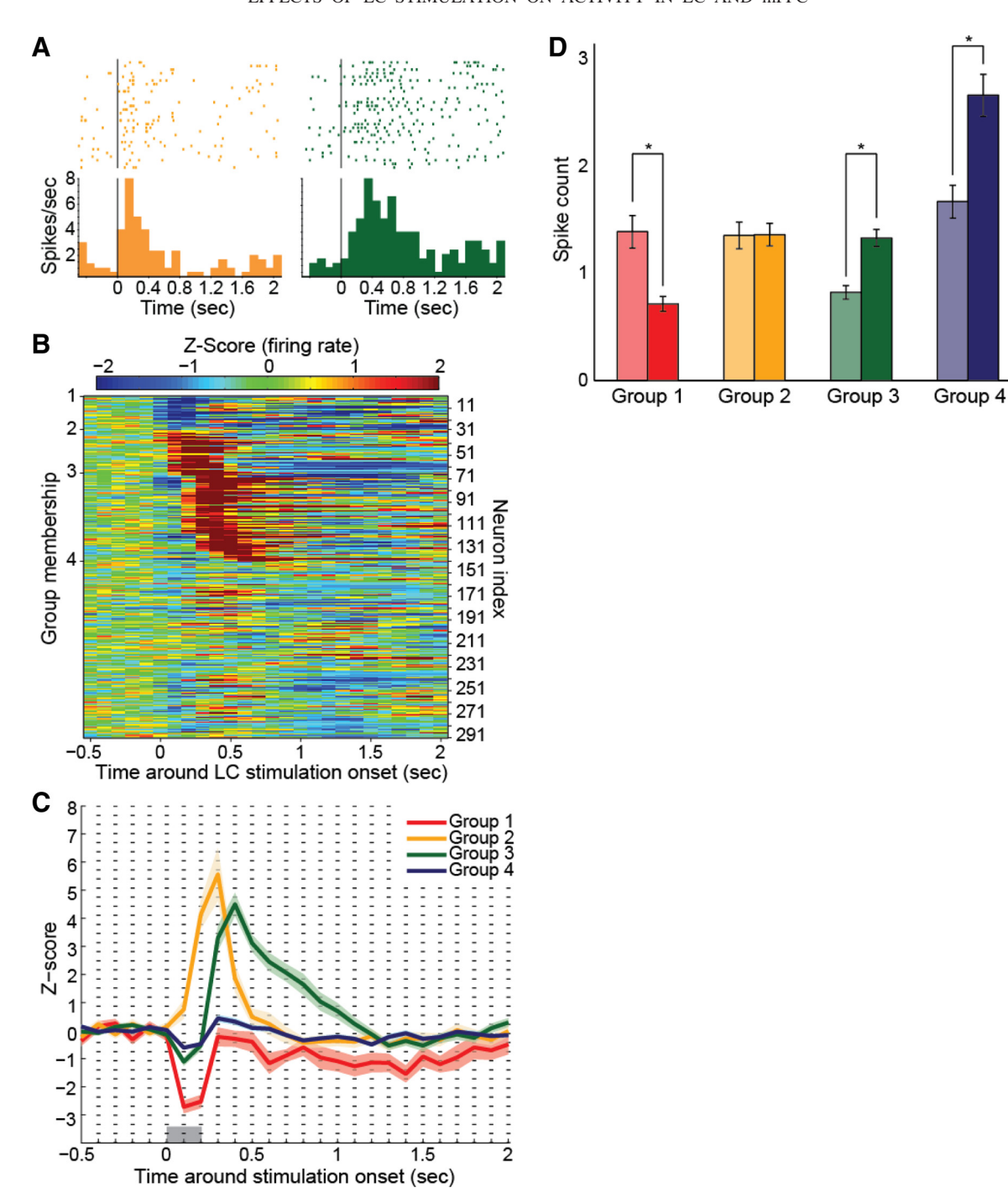


Fig. 10. LC-DES-induced modulation of the firing rate of mPFC single units. A: example single-unit spike raster plots and corresponding PSTHs for a *group* 2 unit (*left*) and a *group* 3 unit (*right*). Both units were excited by LC-DES, but with different time courses. B: normalized (Z score) firing rate of mPFC units (n = 291) recorded during the strongest LC-DES condition (0.4 ms, 0.03- to 0.05-mA pulses at 50 Hz for 200 ms). *Group* 1 units were transiently inhibited immediately after LC-DES, while *group* 2 units were transiently excited. *Group* 3 units were characterized by a delayed and sustained (\sim 1 s) excitation. *Group* 4 units did not meet criteria for significant modulation of the firing rate. C: normalized firing rate for each group of mPFC units in response to the strongest LC-DES as shown in B. D: total spike count during the 500 ms after LC-DES onset (0.4 ms, 0.03- to 0.05-mA pulses at 50 Hz for 200 ms) for the lowest (lighter bars) and highest (darker bars) quartiles of the cortical activation index (see METHODS for more details). Note that the responsiveness of mPFC single units was greater in trials when LC-DES produced a higher level of the cortical population activation. *P < 0.0001 (paired t-test with unequal variances).

neurons and that stronger currents affected activity of almost the entire LC nucleus; nonetheless, SP-DES did not modulate neural activity in the mPFC. In contrast, application of pulse trains, which may have mimicked naturalistic LC bursts and also produced bilateral LC rebound excitation, did modulate cortical activity. We found that populations of mPFC neurons were inhibited or excited by LC-DES. In some mPFC neurons (groups 1 and 2), the firing rate modulation had a relatively short (\sim 100 ms) onset latency and the activity returned to prestimulation level \sim 100 ms after stimulation offset. Another group of mPFC neurons (group 3; 9–26%) increased spiking probability \sim 200 ms after LC-DES offset and remained ex-

Table 4. Number and proportion of mPFC neurons of each group according to LC stimulation condition

DES Frequency	DES Duration	$n_{ m total}$	Group 1 (inhibition)	Group 2 (early excitation)	Group 3 (late excitation)	Group 4 (no change)
20Hz	50 ms	266	13 (4.9)	34 (12.8)	23 (8.7)	196 (73.7)
	100ms	264	15 (5.7)	24 (9.1)	17 (6.4)	208 (78.8)
	200ms	265	13 (4.9)	33 (12.5)	32 (12.1)	187 (70.6)
50Hz	50 ms	319	30 (9.4)	59 (18.5)	24 (7.5)	206 (64.6)
	100ms	316	28 (8.9)	57 (18.0)	49 (15.5)	182 (57.6)
	200ms	291	29 (10.0)	37 (12.7)	75 (25.8)	150 (51.6)

Values are number and proportion (in parentheses) of medial prefrontal cortex (mPFC) neurons for indicated DES conditions.

cited for up to 700 ms. The magnitude of response modulation correlated with the strength of LC-DES parameters in all groups of mPFC neurons.

We found a substantially lower proportion of inhibited mPFC units (5–10%) compared with previous studies, which reported inhibition of \sim 50% of cortical neurons (Dillier et al. 1978; Mantz et al. 1988; Olpe et al. 1980; Phillis and Kostopoulos 1977; Sato et al. 1989). The discrepancy of the results could be due to the milder LC-DES in the present study or

Time around LC stimulation onset (sec)

cortical regional specificity. In contrast, we found a larger proportion of excited units (16-39% combining group 2 and 3 units). Thus the LC-DES parameters employed here resulted in a shift of the excitatory/inhibitory balance of the mPFC to a more excitable state, which was also reflected in a transient (~ 1 s) LFP desynchronization. Moreover, the mPFC neuronal responsiveness to LC-DES was proportional to the overall level of cortical population activation. These results imply that, in the behaving animal, the responsiveness of a single neuron

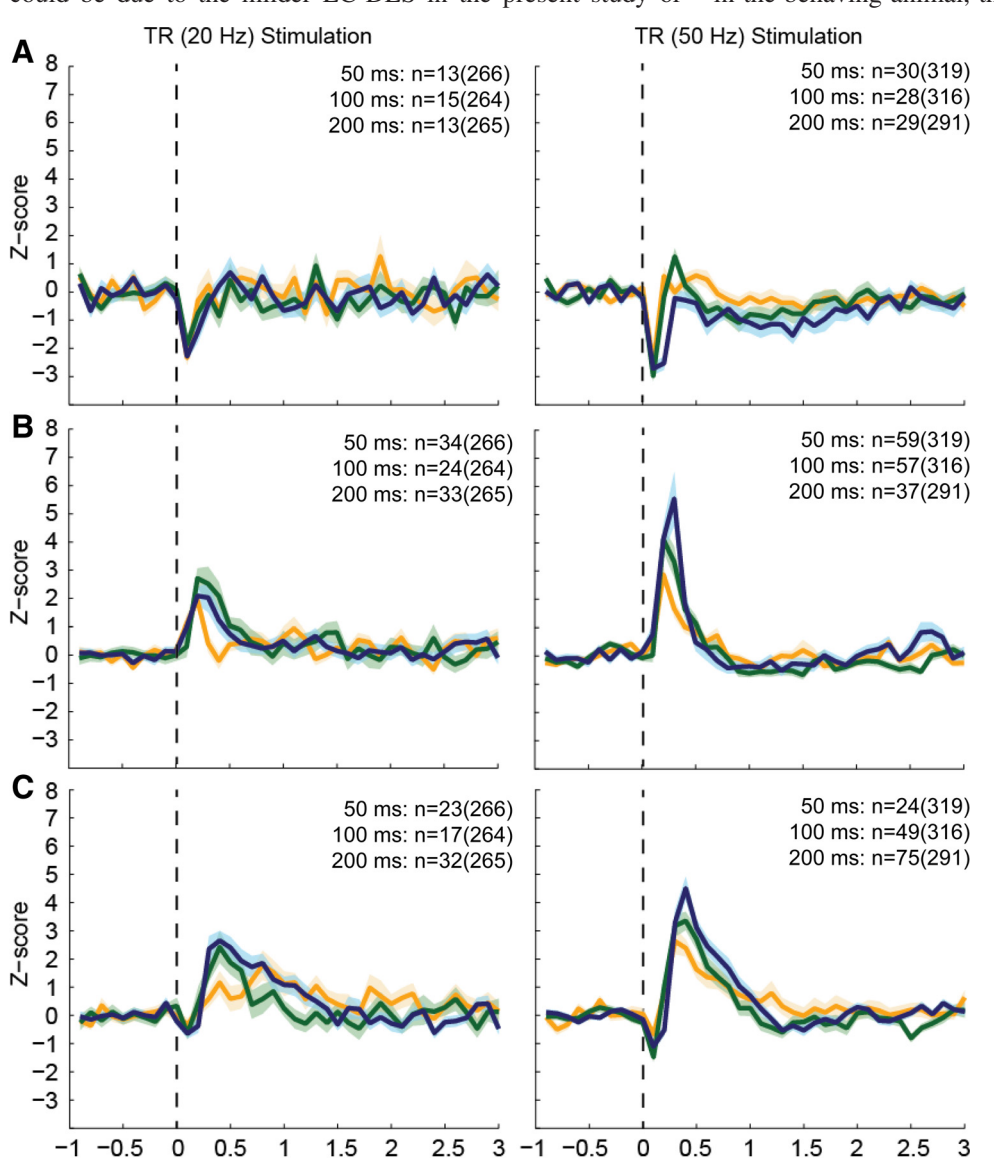


Fig. 11. Modulation of mPFC single-unit responses as a function of LC-DES parameters. Mean ± SE normalized firing rate (Z score) is plotted for each group of responsive units. Group 1 units (A) were inhibited, group 2 units (B) were transiently excited, and group 3 units (C) were excited with a delay and for a longer time. The response to different TR-DES durations is shown by different line colors: orange, 50 ms; green, 100 ms; blue, 200 ms. Data are shown for 20-Hz stimulation (left) and 50-Hz stimulation (right). The number of responsive units out of the total number of units tested for each experimental condition is indicated. For all groups of units, the duration of change in firing rate was proportional to the duration of LC stimulation. Note that 50-Hz stimulation was more effective.

J Neurophysiol • doi:10.1152/jn.00920.2013 • www.jn.org

Time around LC stimulation onset (sec)

will be more strongly modulated by NE if the neuron is within a currently activated large-scale network, as might transiently occur during particular periods of behavioral task performance. Testing this prediction in the future will bring new insights on the regional specificity of the effects of NE in relation to the discrete cognitive functions of a particular brain region or neuronal network.

LC-DES induced sustained activation of mPFC neuronal networks. The dynamics of mPFC unit responses suggest that LC phasic activity may contribute to both fast and slow modulation of mPFC activity. The "fast" (<300 ms) LC modulatory route drives the excitatory response of group 2 units (fast, transient excitation), which in turn excite group 3 units (delayed, sustained excitation) via cortico-cortical or cortico-thalamo-cortical excitatory connections (Constantinople and Bruno 2011; Hirata and Castro-Alamancos 2010; McCormick et al. 1991). The time course of sustained excitation of mPFC single units fits with accompanying changes in the LFP signal indicating transition from the synchronized to desynchronized cortical state. The sustained group 3 singleunit and MUA excitation and LFP desynchronization may reflect the "slow" modulatory route. Thus the NE release in cortex and/or thalamus caused by LC-DES may support cortical recurrent activation (i.e., "slow" modulation), which is a neuronal correlate of working memory (Durstewitz and Seamans 2006; Goldman-Rakic 1995; Wang 2001). It is therefore important to note that iontophoresis of NE receptor agonists and antagonists can modulate cortical sustained spiking activity (Birnbaum et al. 2004; Huang et al. 2007; Sawaguchi 1998), and NE drugs affect working memory in humans and animals (Arnsten 2011).

Indeed, there is extensive evidence that the LC-NE system is involved in promotion and regulation of behavioral arousal (Berridge 2008). It has been long known that naturally occurring (Aston-Jones and Bloom 1981) or experimentally induced LC activation desynchronizes cortical EEG (Berridge and Foote 1991; Dringenberg and Vanderwolf 1998; 1997; Olpe et al. 1980). Unlike previous studies that mainly described effects of tonic LC activation, we focused here on phasic LC activation by applying brief (50-200 ms) pulse trains, which model the LC burst firing in response to alerting stimuli. Our results indicate that a series of pulses presented at 50 Hz for 200 ms (total 11 pulses) was sufficient to shift the cortical state under urethane anesthesia. Our findings further support earlier studies demonstrating that LC spontaneous spiking is related to cortical excitability state in both behaving and anesthetized rats (Eschenko et al. 2012; Lestienne et al. 1997). Spontaneous fluctuations of cortical excitability under anesthesia have been commonly used as a model for the natural level of network activity during alert states (Constantinople and Bruno 2011; Harris and Thiele 2011; Hasenstaub et al. 2007). Clearly, the dynamic properties of cortical excitability may differ in behaving animals, but we expect that LC phasic activation, caused by a feedforward or top-down excitatory input, may result in similar changes in cortical excitability as reported in the present study.

The modulation of mPFC excitability state could be a result of NE release directly in mPFC (Constantinople and Bruno 2011), in thalamus (Hirata and Castro-Alamancos 2010), or mediated by LC-DES-induced activation of cholinergic ascending pathways (Berridge and Wifler 2000; Dringenberg and Vanderwolf 1997, 1998; Manns et al. 2003; Mena-Segovia and

Bolam 2011). It has been shown that EEG desynchronization induced by LC activation can be blocked by cholinergic antagonists (Dringenberg and Vanderwolf 1997) or by blocking postsynaptic β -adrenergic receptors in the basal forebrain (Berridge and Wifler 2000). It has been also suggested that NE promotes an active cortical state by inhibiting GABAergic neurons in the nucleus basalis via α_2 -adrenergic receptors (Manns et al. 2003). Recently, it has been demonstrated that optogenetic activation of cholinergic neurons of the basal forebrain results in cortical desynchronization (Pinto et al. 2013). In our own experiments, we also observed that LC-DES-induced cortical activation could be blocked by systemic administration of clonidine (0.05 mg/kg ip) or scopolamine (5 mg/kg ip; data not shown). We assume that the observed effect of clonidine was due to overall reduced NE transmission in the brain, while the DES-induced phasic NE release was most likely present. This assumption is based on our (unpublished) observations that despite the substantial suppression of LC spontaneous activity by clonidine, the phasic discharge of LC-NE neurons in response to a strong excitatory input, for example noxious stimulation, is preserved.

Thus cortical effects reported in the present study are likely mediated by multiple mechanisms that were triggered by LC phasic activation. Further investigations may identify the exact nature of interactions between LC phasic activation and other brain regions controlling cortical state.

LC-DES probes central NE modulation of prefrontal function. We demonstrated that mild unilateral LC-DES elicits a biphasic response of LC-NE neurons bilaterally, which implies modulation of LC forebrain targets bilaterally due to associated NE release (Berridge and Abercrombie 1999; Florin-Lechner et al. 1996; Tanaka et al. 1976). The fact that LC phasic activation by DES produced a biphasic response of NE neurons resembling a naturalistic LC response to a salient stimulus in behaving animals (Aston-Jones et al. 1991a; Bouret and Richmond 2009; Bouret and Sara 2004; Foote et al. 1980) makes DES a useful tool for probing the effects of phasic LC activity on cortical state and the behavioral consequences of such activation (Sara and Devauges 1988). Numerous behavioral studies have demonstrated the essential role of NE transmission in mPFC-mediated cognitive functions such as attention, working memory, and cognitive flexibility (Arnsten 2011; Sara 2009). It has been suggested that the LC phasic response may contribute to "resetting" or "tuning" cortical neurons so that they process information more efficiently (Berridge and Waterhouse 2003; Bouret and Sara 2005; Harris and Thiele 2011; Sara 2009). We have described activation of mPFC putative pyramidal neurons and a population shift to a more excitable state produced by LC-DES. This sustained (~ 1 s or more) period of cortical activation may support optimal cortical processing according to attention or working memory demands (Arnsten 2011; Goldman-Rakic 1995; Totah et al. 2009). Both the fast "reset" of cortical state and sustained activation may be supported by the phasic activation of the LC-NE system.

Concluding remarks on LC-DES specificity. The selectivity of DES has always been and continues to be a debated issue (Borchers et al. 2012; Logothetis et al. 2010). Neither the passive current spread nor the identity of excited elements can be fully determined for a given current density, although studies of excitability (e.g., calculation of rheobase and chronaxie for any given stimulation site) provide an estimation of

the current spread and excited population (Tehovnik et al. 2006). In certain conditions optimal selectivity can be achieved by using the newly developed optogenetic tools, yet the actual selectivity of the latter method depends on the microconnectivity of a given structure. In cortex, for instance, the strongly recurrent connectivity underlies both signal amplification and balance between excitation and inhibition; therefore optogenetic stimulation has virtual selectivity indeed. Selective activation of a particular neuronal group will unavoidably result in instant activation of the entire local network (Logothetis 2010). Taking into account the widespread distal and local LC connectivity, application of either optogenetic or DES stimulation will not, for example, prevent orthodromic activation of the multiple direct targets of LC, which may or may not take place during naturalistic LC discharge. Optogenetic stimulation will undoubtedly spare antidromic activation of fibers, and it may prove useful to compare the connectivity patterns induced by the two methodologies in the near future. Yet DES remains a valuable experimental tool with great translational value. Better understanding the local and distal effects of DES in general, besides extending basic scientific knowledge, has important clinical relevance.

ACKNOWLEDGMENTS

We thank David Omer, Stefano Panzeri, Susan Sara, and Silvia van Keulen for valuable comments on the manuscript and Axel Oeltermann and Joachim Werner for technical support.

Present address of A. Marzo: Research Dept. of Cell and Developmental Biology, University College London, London, UK.

GRANTS

This work was supported by the Fyssen Foundation for postdoctoral study (A. Marzo) and the SI-CODE project of the Future and Emerging Technologies (FET) Programme within the 7th Framework Programme for Research of the European Commission, under FET-Open Grant FP7-284553 (N. K. Totah, N. K. Logothetis, and O. Eschenko).

DISCLOSURES

No conflicts of interest, financial or otherwise, are declared by the author(s).

AUTHOR CONTRIBUTIONS

Author contributions: A.M. and R.M.N. performed experiments; A.M., N.K.T., R.M.N., and O.E. analyzed data; A.M., N.K.T., R.M.N., N.K.L., and O.E. interpreted results of experiments; A.M., N.K.T., and O.E. drafted manuscript; A.M., N.K.T., R.M.N., N.K.L., and O.E. edited and revised manuscript; A.M., N.K.T., R.M.N., N.K.L., and O.E. approved final version of manuscript; N.K.T., R.M.N., and O.E. prepared figures; N.K.L. and O.E. conception and design of research.

REFERENCES

- **Aghajanian G, VanderMaelen C.** Alpha 2-adrenoceptor-mediated hyperpolarization of locus coeruleus neurons: intracellular studies in vivo. *Science* 215: 1394–1396, 1982.
- **Aghajanian GK, Cedarbaum JM, Wang RY.** Evidence for norepinephrine-mediated collateral inhibition of locus coeruleus neurons. *Brain Res* 136: 570–577, 1977.
- **Arnsten AF.** Catecholamine influences on dorsolateral prefrontal cortical networks. *Biol Psychiatry* 69: e89–e99, 2011.
- **Aston-Jones G, Bloom FE.** Activity of norepinephrine-containing locus coeruleus neurons in behaving rats anticipates fluctuations in the sleepwaking cycle. *J Neurosci* 1: 876–886, 1981.
- **Aston-Jones G, Chiang C, Alexinsky T.** Discharge of noradrenergic locus coeruleus neurons in behaving rats and monkeys suggests a role in vigilance. *Prog Brain Res* 88: 501–520, 1991a.

- **Aston-Jones G, Cohen JD.** An integrative theory of locus coeruleus-norepinephrine function: adaptive gain and optimal performance. *Annu Rev Neurosci* 28: 403–450, 2005.
- **Aston-Jones G, Ennis M, Pieribone VA, Nickell WT, Shipley MT.** The brain nucleus locus coeruleus: restricted afferent control of a broad efferent network. *Science* 234: 734–737, 1986.
- **Aston-Jones G, Gold JI.** How we say no: norepinephrine, inferior frontal gyrus, and response inhibition. *Biol Psychiatry* 65: 548–549, 2009.
- **Aston-Jones G, Rajkowski J, Kubiak P, Alexinsky T.** Locus coeruleus neurons in monkey are selectively activated by attended cues in a vigilance task. *J Neurosci* 14: 4467–4480, 1994.
- Aston-Jones G, Shipley MT, Chouvet G, Ennis M, van Bockstaele E, Pieribone V, Shiekhattar R, Akaoka H, Drolet G, Astier B, Charlety P, Valentino R, Williams JT. Afferent regulation of locus coeruleus neurons: anatomy, physiology and pharmacology. *Prog Brain Res* 88: 47–75, 1991b.
- Aston-Jones G, Zhu Y, Card JP. Numerous GABAergic afferents to locus ceruleus in the pericerulear dendritic zone: possible interneuronal pool. J Neurosci 24: 2313–2321, 2004.
- **Beaudet A, Descarries L.** The monoamine innervation of rat cerebral cortex: synaptic and nonsynaptic axon terminals. *Neuroscience* 3: 851–860, 1978.
- Belitski A, Gretton A, Magri C, Murayama Y, Montemurro MA, Logothetis NK, Panzeri S. Low-frequency local field potentials and spikes in primary visual cortex convey independent visual information. J Neurosci 28: 5696–5709, 2008.
- Berridge CW. Noradrenergic modulation of arousal. Brain Res Rev 58: 1–17, 2008.
 Berridge CW, Abercrombie ED. Relationship between locus coeruleus discharge rates and rates of norepinephrine release within neocortex as assessed by in vivo microdialysis. Neuroscience 93: 1263–1270, 1999.
- Berridge CW, Foote SL. Effects of locus coeruleus activation on electroencephalographic activity in neocortex and hippocampus. J Neurosci 11: 3135–3145, 1991.
- Berridge CW, Waterhouse BD. The locus coeruleus-noradrenergic system: modulation of behavioral state and state-dependent cognitive processes. *Brain Res Brain Res Rev* 42: 33–84, 2003.
- Berridge CW, Wifler K. Contrasting effects of noradrenergic β-receptor blockade within the medial septal area on forebrain electroencephalographic and behavioral activity state in anesthetized and unanesthetized rat. *Neuroscience* 97: 543–552, 2000.
- Birnbaum SG, Yuan PX, Wang M, Vijayraghavan S, Bloom AK, Davis DJ, Gobeske KT, Sweatt JD, Manji HK, Arnsten AF. Protein kinase C overactivity impairs prefrontal cortical regulation of working memory. *Science* 306: 882–884, 2004.
- Borchers S, Himmelbach M, Logothetis N, Karnath HO. Direct electrical stimulation of human cortex: the gold standard for mapping brain functions? *Nat Rev* 13: 63–70. 2012.
- **Bouret S, Richmond BJ.** Relation of locus coeruleus neurons in monkeys to Pavlovian and operant behaviors. *J Neurophysiol* 101: 898–911, 2009.
- **Bouret S, Sara SJ.** Locus coeruleus activation modulates firing rate and temporal organization of odour-induced single-cell responses in rat piriform cortex. *Eur J Neurosci* 16: 2371–2382, 2002.
- **Bouret S, Sara SJ.** Reward expectation, orientation of attention and locus coeruleus-medial frontal cortex interplay during learning. *Eur J Neurosci* 20: 791–802, 2004.
- **Bouret S, Sara SJ.** Network reset: a simplified overarching theory of locus coeruleus noradrenaline function. *Trends Neurosci* 28: 574–582, 2005.
- Branchereau P, Van Bockstaele EJ, Chan J, Pickel VM. Pyramidal neurons in rat prefrontal cortex show a complex synaptic response to single electrical stimulation of the locus coeruleus region: evidence for antidromic activation and GABAergic inhibition using in vivo intracellular recording and electron microscopy. *Synapse* 22: 313–331, 1996.
- Butovas S, Schwarz C. Spatiotemporal effects of microstimulation in rat neocortex: a parametric study using multielectrode recordings. *J Neuro*physiol 90: 3024–3039, 2003.
- Cedarbaum JM, Aghajanian GK. Activation of locus coeruleus neurons by peripheral stimuli: modulation by a collateral inhibitory mechanism. *Life Sci* 23: 1383–1392, 1978.
- Chen FJ, Sara SJ. Locus coeruleus activation by foot shock or electrical stimulation inhibits amygdala neurons. *Neuroscience* 144: 472–481, 2007.
- Clement EA, Richard A, Thwaites M, Ailon J, Peters S, Dickson CT. Cyclic and sleep-like spontaneous alternations of brain state under urethane anaesthesia. PLoS One 3: e2004, 2008.
- Cohen MR, Newsome WT. What electrical microstimulation has revealed about the neural basis of cognition. Curr Opin Neurobiol 14: 169–177, 2004.
- Constantinople CM, Bruno RM. Effects and mechanisms of wakefulness on local cortical networks. *Neuron* 69: 1061–1068, 2011.

- Curto C, Sakata S, Marguet S, Itskov V, Harris KD. A simple model of cortical dynamics explains variability and state dependence of sensory responses in urethane-anesthetized auditory cortex. *J Neurosci* 29: 10600–10612, 2009.
- Dayan P, Yu AJ. Phasic norepinephrine: a neural interrupt signal for unexpected events. *Network* 17: 335–350, 2006.
- **Devilbiss DM, Page ME, Waterhouse BD.** Locus ceruleus regulates sensory encoding by neurons and networks in waking animals. *J Neurosci* 26: 9860–9872, 2006.
- **Devilbiss DM, Waterhouse BD.** Phasic and tonic patterns of locus coeruleus output differentially modulate sensory network function in the awake rat. *J Neurophysiol* 105: 69–87, 2011.
- **Devoto P, Flore G, Saba P, Fà M, Gessa GL.** Stimulation of the locus coeruleus elicits noradrenaline and dopamine release in the medial prefrontal and parietal cortex. *J Neurochem* 92: 368–374, 2005.
- **Dillier N, Laszlo J, Muller B, Koella WP, Olpe HR.** Activation of an inhibitory noradrenergic pathway projecting from the locus coeruleus to the cingulate cortex of the rat. *Brain Res* 154: 61–68, 1978.
- **Dringenberg HC, Vanderwolf CH.** Neocortical activation: modulation by multiple pathways acting on central cholinergic and serotonergic systems. *Exp Brain Res* 116: 160–174, 1997.
- Dringenberg HC, Vanderwolf CH. Involvement of direct and indirect pathways in electrocorticographic activation. Neurosci Biobehav Rev 22: 243–257, 1998.
- Durstewitz D, Seamans JK. Beyond bistability: biophysics and temporal dynamics of working memory. *Neuroscience* 139: 119–133, 2006.
- Ennis M, Aston-Jones G. Evidence for self- and neighbor-mediated postactivation inhibition of locus coeruleus neurons. *Brain Res* 374: 299–305, 1986.
- Ennis M, Aston-Jones G. GABA-mediated inhibition of locus coeruleus from the dorsomedial rostral medulla. *J Neurosci* 9: 2973–2981, 1989.
- Ennis M, Aston-Jones G, Shiekhattar R. Activation of locus coeruleus neurons by nucleus paragigantocellularis or noxious sensory stimulation is mediated by intracoerulear excitatory amino acid neurotransmission. *Brain Res* 598: 185–195, 1992.
- Eschenko O, Magri C, Panzeri S, Sara SJ. Noradrenergic neurons of the locus coeruleus are phase locked to cortical up-down states during sleep. *Cereb Cortex* 22: 426–435, 2012.
- **Florin-Lechner SM, Druhan JP, Aston-Jones G, Valentino RJ.** Enhanced norepinephrine release in prefrontal cortex with burst stimulation of the locus coeruleus. *Brain Res* 742: 89–97, 1996.
- **Foote SL, Aston-Jones G, Bloom FE.** Impulse activity of locus coeruleus neurons in awake rats and monkeys is a function of sensory stimulation and arousal. *Proc Natl Acad Sci USA* 77: 3033–3037, 1980.
- Goldman-Rakic PS. Cellular basis of working memory. Neuron 14: 477–485, 1995.
- Grill WM, Snyder AN, Miocinovic S. Deep brain stimulation creates an informational lesion of the stimulated nucleus. *Neuroreport* 15: 1137–1140, 2004.
- **Groves DA, Bowman EM, Brown VJ.** Recordings from the rat locus coeruleus during acute vagal nerve stimulation in the anaesthetised rat. *Neurosci Lett* 379: 174–179, 2005.
- Harris KD, Thiele A. Cortical state and attention. *Nat Rev* 12: 509–523, 2011.
 Hasenstaub A, Sachdev RN, McCormick DA. State changes rapidly modulate cortical neuronal responsiveness. *J Neurosci* 27: 9607–9622, 2007.
- Hermans EJ, van Marle HJ, Ossewaarde L, Henckens MJ, Qin S, van Kesteren MT, Schoots VC, Cousijn H, Rijpkema M, Oostenveld R, Fernández G. Stress-related noradrenergic activity prompts large-scale neural network reconfiguration. *Science* 334: 1151–1153, 2011.
- **Hirata A, Castro-Alamancos MA.** Neocortex network activation and deactivation states controlled by the thalamus. *J Neurophysiol* 103: 1147–1157, 2010.
- **Histed MH, Bonin V, Reid RC.** Direct activation of sparse, distributed populations of cortical neurons by electrical microstimulation. *Neuron* 63: 508–522, 2009.
- Huang HP, Wang SR, Yao W, Zhang C, Zhou Y, Chen XW, Zhang B, Xiong W, Wang LY, Zheng LH, Landry M, Hökfelt T, Xu ZQ, Zhou Z. Long latency of evoked quantal transmitter release from somata of locus coeruleus neurons in rat pontine slices. *Proc Natl Acad Sci USA* 104: 1401–1406, 2007.
- **Jones BE, Moore RY.** Ascending projections of the locus coeruleus in the rat. II. Autoradiographic study. *Brain Res* 127: 25–53, 1977.
- Kayama Y, Sato H. Effects of locus coeruleus stimulation on neuronal activities in the rat superior colliculus. Jpn J Physiol 32: 1011–1014, 1982.
- Langer SZ. Presynaptic regulation of the release of catecholamines. *Pharma-col Rev* 32: 337–362, 1980.
- Lecas JC. Locus coeruleus activation shortens synaptic drive while decreasing spike latency and jitter in sensorimotor cortex. Implications for neuronal integration. Eur J Neurosci 19: 2519–2530, 2004.

- **Lestienne R, Herve-Minvielle A, Robinson D, Briois L, Sara SJ.** Slow oscillations as a probe of the dynamics of the locus coeruleus-frontal cortex interaction in anesthetized rats. *J Physiol Paris* 91: 273–284, 1997.
- **Lindvall O, Björklund A, Divac I.** Organization of catecholamine neurons projecting to the frontal cortex in the rat. *Brain Res* 142: 1–24, 1978.
- **Logothetis NK.** The underpinnings of the BOLD functional magnetic resonance imaging signal. *J Neurosci* 23: 3963–3971, 2003.
- Logothetis NK. Bold claims for optogenetics. Nature 468: E3-E5, 2010.
- Logothetis NK, Augath M, Murayama Y, Rauch A, Sultan F, Goense J, Oeltermann A, Merkle H. The effects of electrical microstimulation on cortical signal propagation. *Nat Neurosci* 13: 1283–1291, 2010.
- Luppi PH, Aston-Jones G, Akaoka H, Chouvet G, Jouvet M. Afferent projections to the rat locus coeruleus demonstrated by retrograde and anterograde tracing with cholera-toxin B subunit and *Phaseolus vulgaris* leucoagglutinin. *Neuroscience* 65: 119–160, 1995.
- Manns ID, Lee MG, Modirrousta M, Hou YP, Jones BE. Alpha 2 adrenergic receptors on GABAergic, putative sleep-promoting basal forebrain neurons. *Eur J Neurosci* 18: 723–727, 2003.
- Mantz J, Milla C, Glowinski J, Thierry AM. Differential effects of ascending neurons containing dopamine and noradrenaline in the control of spontaneous activity and of evoked responses in the rat prefrontal cortex. *Neuroscience* 27: 517–526, 1988.
- McCormick DA, Pape HC, Williamson A. Actions of norepinephrine in the cerebral cortex and thalamus: implications for function of the central noradrenergic system. *Prog Brain Res* 88: 293–305, 1991.
- **Mena-Segovia J, Bolam JP.** Phasic modulation of cortical high-frequency oscillations by pedunculopontine neurons. *Prog Brain Res* 193: 85–92, 2011.
- Moore RY, Bloom FE. Central catecholamine neuron systems: anatomy and physiology of the norepinephrine and epinephrine systems. Annu Rev Neurosci 2: 113–168, 1979.
- **Olpe HR, Glatt A, Laszlo J, Schellenberg A.** Some electrophysiological and pharmacological properties of the cortical, noradrenergic projection of the locus coeruleus in the rat. *Brain Res* 186: 9–19, 1980.
- **Paxinos G, Watson C.** *The Rat Brain in Stereotaxic Coordinates.* Amsterdam: Elsevier Academic, 2005.
- **Phillis JW, Kostopoulos GK.** Activation of a noradrenergic pathway from the brain stem to rat cerebral cortex. *Gen Pharmacol* 8: 207–211, 1977.
- Pinto L, Goard MJ, Estandian D, Xu M, Kwan AC, Lee SH, Harrison TC, Feng G, Dan Y. Fast modulation of visual perception by basal forebrain cholinergic neurons. *Nat Neurosci* 16: 1857–1863, 2013.
- Ranck JB Jr. Which elements are excited in electrical stimulation of mammalian central nervous system: a review. *Brain Res* 98: 417–440, 1975.
- Sara SJ. The locus coeruleus and noradrenergic modulation of cognition. *Nat Rev* 10: 211–223, 2009.
- Sara SJ, Devauges V. Priming stimulation of locus coeruleus facilitates memory retrieval in the rat. *Brain Res* 438: 299–303, 1988.
- Sato H, Fox K, Daw NW. Effect of electrical stimulation of locus coeruleus on the activity of neurons in the cat visual cortex. J Neurophysiol 62: 946–958, 1989.
- Sawaguchi T. Attenuation of delay-period activity of monkey prefrontal neurons by an alpha2-adrenergic antagonist during an oculomotor delayed-
- response task. *J Neurophysiol* 80: 2200–2205, 1998. **Snow PJ, Andre P, Pompeiano O.** Effects of locus coeruleus stimulation on the responses of SI neurons of the rat to controlled natural and electrical stimulation of the skin. *Arch Ital Biol* 137: 1–28, 1999.
- **Steriade M, Contreras D, Curro Dossi R, Nunez A.** The slow (<1 Hz) oscillation in reticular thalamic and thalamocortical neurons: scenario of sleep rhythm generation in interacting thalamic and neocortical networks. *J Neurosci* 13: 3284–3299, 1993.
- Tanaka C, Inagaki C, Fujiwara H. Labeled noradrenaline release from rat cerebral cortex following electrical stimulation of locus coeruleus. *Brain Res* 106: 384–389, 1976.
- **Tehovnik EJ, Tolias AS, Sultan F, Slocum WM, Logothetis NK.** Direct and indirect activation of cortical neurons by electrical microstimulation. *J Neurophysiol* 96: 512–521, 2006.
- **Totah NK, Kim YB, Homayoun H, Moghaddam B.** Anterior cingulate neurons represent errors and preparatory attention within the same behavioral sequence. *J Neurosci* 29: 6418–6426, 2009.
- Wang XJ. Synaptic reverberation underlying mnemonic persistent activity. Trends Neurosci 24: 455–463, 2001.
- Watabe K, Satoh T. Mechanism underlying prolonged inhibition of rat locus coeruleus neurons following anti- and orthodromic activation. *Brain Res* 165: 343–347, 1979.